http://doi.org/10.1093/plcell/koab285 THE PLANT CELL 2022: 34: 1621–1640

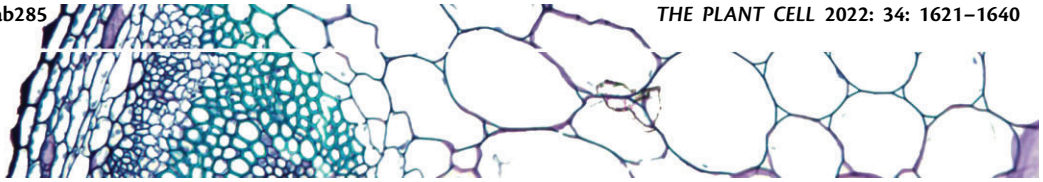

Research Article

The N-terminally truncated helper NLR *NRG1C* antagonizes immunity mediated by its full-length neighbors *NRG1A* and *NRG1B*

Zhongshou Wu [1,2], **Lei Tian** [1,2], **Xueru Liu** [1,2], **Weijie Huang** [2], **Yuelin Zhang** [2] and **Xin Li** [1,2,*,†]

1 Michael Smith Laboratories, University of British Columbia, Vancouver, BC V6T 1Z4, Canada
2 Department of Botany, University of British Columbia, Vancouver, BC V6T 1Z4, Canada

*Author for correspondence: xinli@msl.ubc.ca
†Senior author.
These authors contributed equally (Z.W., L.T.).
Z.W., Data curation, Validation, Investigation, Methodology, Writing—original draft, Project administration; L.T., Validation, Methodology, Writing; X.Liu, Validation, Methodology; W.H., Validation, Methodology; Y.Z., Formal analysis, Supervision, Funding acquisition; X.L., Conceptualization, Data curation, Formal analysis, Supervision, Funding acquisition, Writing—original draft, Project administration, Writing—revisions. All authors reviewed the manuscript.
The author responsible for distribution of materials integral to the findings presented in this article in accordance with the policy described in the Instructions for Authors is (https://academic.oup.com/plcell): Xin Li (xinli@msl.ubc.ca)

Abstract

Both plants and animals utilize nucleotide-binding leucine-rich repeat immune receptors (NLRs) to perceive the presence of pathogen-derived molecules and induce immune responses. *NLR* genes are far more abundant and diverse in vascular plants than in animals. Truncated NLRs, which lack one or more of the canonical domains, are also commonly encoded in plant genomes. However, little is known about their functions, especially the N-terminally truncated ones. Here, we show that the *Arabidopsis thaliana* N-terminally truncated helper NLR (hNLR) gene *N REQUIREMENT GENE1 (NRG1C)* is highly induced upon pathogen infection and in autoimmune mutants. The immune response and cell death conferred by some Toll/interleukin-1 receptor-type NLRs (TNLs) were compromised in Arabidopsis *NRG1C* overexpression lines. Detailed genetic analysis revealed that *NRG1C* antagonizes the immunity mediated by its full-length neighbors *NRG1A* and *NRG1B*. Biochemical tests suggested that NRG1C might interfere with the EDS1–SAG101 complex, which functions in immunity signaling together with NRG1A/1B. Interestingly, Brassicaceae NRG1Cs are functionally exchangeable and that the *Nicotiana benthamiana* N-terminally truncated hNLR NRG2 also antagonizes NRG1 activity. Together, our study uncovers an unexpected negative role of N-terminally truncated hNLRs in immunity in different plant species.

Introduction

Plants utilize a sophisticated innate immune system to defend against a plethora of pathogens. They depend on immune receptors to recognize nonself signals and initiate defense responses. Plasma membrane-localized pattern-recognition receptors (PRRs) perceive pathogen-associated molecular patterns (PAMPs), leading to PAMP/pattern-triggered immunity (Couto and Zipfel, 2016). On the other hand, intracellular nucleotide-binding (NB) leucine-rich repeat (LRR) immune receptors (NLRs) are responsible for warding off adapted

Received September 14, 2021. Accepted November 11, 2021. Advance access publication November 19, 2021

IN A NUTSHELL

Background: Plants utilize sophisticated innate immune systems to fight against pathogens. Their genomes encode abundant immune receptors to detect the presence of pathogens and initiate defense responses. Nucleotide-binding leucine-rich repeat immune receptors (NLRs) constitute a major type of immune receptor, which are also present in animals. NLRs with pathogen recognition ability are sensor NLRs (sNLRs), whereas those required for sNLR-mediated defense are helper NLRs (hNLRs). NRG1 (N REQUIREMENT GENE1) family proteins are hNLRs that function with two lipase-like proteins, EDS1 (ENHANCED DISEASE SUSCEPTIBILITY1) and SAG101 (SENESCENCE-ASSOCIATED GENE 101), downstream of some sNLRs. Interestingly, N-terminally truncated *NRG1C* is clustered in tandem with full-length *NRG1s* in Brassicaceae genomes. However, little is known about the function of NRG1C in plant immunity.

Question: We asked whether N-terminally truncated NRG1C plays a role in plant immunity. If so, what is the molecular mechanism?

Findings: Using overexpression approaches, we found that NRG1C plays a negative role in plant immunity. Upon pathogen infection, *NRG1C* expression is induced. Furthermore, NRG1C antagonizes immunity mediated by the sNLRs that is dependent on full-length NRG1s. However, NRG1C does not affect the transcript or protein levels of full-length NRG1s, and it does not associate with them either. The interaction of NRG1C with EDS1 and SAG101 suggests that it might interfere with the EDS1-SAG101 complex, which signals together with full-length NRG1s.

Next steps: Besides *NRG1C*, other N-terminally truncated *NLR* (*NL*) genes are present in plant genomes. Additional investigations into the functions of such *NL* genes in plants will be of great interest to widen our understanding of plant NLRs and their regulation.

pathogens by detecting their secreted effectors, thereby activating effector-triggered immunity (Cui et al., 2015).

NLRs are present in both animals and plants. They are members of the signal transduction ATPases with numerous domains family, consisting of a variable N-terminal domain, a central NB motif, and a C-terminal LRR region (Jones and Dangl, 2006). Typical plant sensor NLRs (sNLRs) have either a Toll/interleukin-1 receptor (TIR) or a coiled-coil (CC) domain at their N-termini and are termed TNLs (TIR-NB-LRR) or CNLs (CC-NB-LRR), respectively (Jones et al., 2016). NLRs have evolved to recognize effectors directly or indirectly (Baggs et al., 2017). In contrast, a small subclass of NLRs is genetically required for the immune signaling of diverse sNLRs. These NLRs are termed helper NLRs (hNLRs) (Peart et al., 2005; Bonardi et al., 2011; Collier et al., 2011; Jubic et al., 2019). There are two *hNLR* gene families in *Arabidopsis thaliana*, encoding RNLs (Resistance to Powdery Mildew 8 [RPW8] CC-NB-LRR): the *ACTIVATED DISEASE RESISTANCE 1* (*ADR1*) family (Bonardi et al., 2011) and the *N REQUIREMENT GENE 1* (*NRG1*) family (Peart et al., 2005). Besides RNLs, the Solanaceae-specific CNL NRC (NB-LRR protein required for hypersensitive response (HR)-associated cell death) proteins also function as hNLRs, since both cell surface PRRs (Wu et al., 2016; Rathjen and Dodds, 2017) and many sNLRs signal through NRCs (Gabriëls et al., 2006, 2007; Wu et al., 2017a). Compared to the highly divergent sensor TNLs and CNLs, hNLRs are evolutionarily more conserved (Shao et al., 2016; Zhong and Cheng, 2016; Wu et al., 2017a; Adachi et al., 2019; Andolfo et al., 2019).

Plant *sNLRs* are among the most rapidly evolving genes (Guo et al., 2011; Gao et al., 2018; Van de Weyer et al., 2019). As a result, they are highly polymorphic. *NLR* allelic diversity mainly depends on the generation of either chimeric LRRs by intra- and intergenic recombination and gene conversion (Serra et al., 2018), or novel LRRs through point mutations (Michelmore and Meyers, 1998; Mago et al., 2015; Lu et al., 2016; Tamborski and Krasileva, 2020). Gene clustering is another feature commonly observed for plant *NLRs* (Van de Weyer et al., 2019). Two types of cluster patterns exist based on the diversity of *NLRs* within the clusters (Jacob et al., 2013). Homogenous clusters contain the same type of *NLRs* derived from tandem duplications. By contrast, heterogeneous clusters contain diverse *NLRs* generated by ectopic or large-scale segmental duplications (Jacob et al., 2013; Marone et al., 2013; Krasileva, 2019). Pan-genome analysis revealed that *NLR* cluster patterns vary among *A. thaliana* accessions. Some clusters have highly conserved copy numbers, while others show huge variations (Lee and Chae, 2020). An increasing number of examples suggest that clustered *NLR* genes often are co-expressed and may cooperate to function. Clustering *sNLRs* together has the potential to massively expand pathogen recognition by increasing their oligomerization options (van Wersch and Li, 2019).

Duplication and uneven crossover events may generate *NLRs* lacking one or more of the canonical domains, yielding truncated *NLRs* (Wicker et al., 2007; Baggs et al., 2017), which are commonly found in plant genomes (Bai et al., 2002; Meyers et al., 2002; 2003; Yang et al., 2008; Jacob et al., 2013; Van de Weyer et al., 2019; Lee and Chae, 2020). Interesting, most truncated *NLRs* are expressed (Meyers et al., 2002; Tan et al., 2007; Nandety et al., 2013), suggesting their potential role in plant immunity. Several C-terminally truncated NLRs have been studied. For instance, *A. thaliana* TIR-only protein RESPONSE TO HopBA1 (RBA1) is specifically required for

defense responses mediated by the bacterial effector HopBA1 (Nishimura et al., 2017). Another well-studied example involves the *A. thaliana* TN (TIR-NB) proteins CHILLING SENSITIVE1 (CHS1) and TN2. CHS1 and TN2 form distinct pairs with full-length TNL SOC3 (SUPPRESSOR of *chs1-2*, 3) to monitor the homeostasis of the E3 ligase SENESCENCE-ASSOCIATED E3 UBIQUITIN LIGASE 1 (SAUL1) (Tong et al., 2017; Liang et al., 2019). However, little is known about the functions of N-terminally truncated NLRs, including NL (NB-LRR) and LRR proteins.

Although hNLRs may not have effector recognition capabilities, the NRG1-type *hNLRs* are organized in clusters in various plant species (Andolfo et al., 2019; Jubic et al., 2019; van Wersch and Li, 2019; Wu et al., 2019). In contrast, *ADR1s* are scattered in the genome (Bonardi et al., 2011; Dong et al., 2016). There are three *NRG1* paralogs in the *A. thaliana* genome: full-length *NRG1A* and *NRG1B*, and N-terminally truncated *NRG1C* (Jubic et al., 2019; Wu et al., 2019). *NRG1A* and *NRG1B* are present in the *NRG1* cluster across almost all analyzed *A. thaliana* and *A. lyrate* accessions (Lee and Chae, 2020). *NRC1C* encodes a predicted protein missing the RPW8 CC domain and most of the NB domain. Similarly, *Nicotiana benthamiana* contains a copy of the full-length *NRG1* and an N-terminally truncated *NRG2*. In comparison to the clustered *NRG1s* in *A. thaliana*, *NRG2* does not cluster with *NRG1* and has been assumed to be a pseudogene (Peart et al., 2005). It is unclear whether these N-terminally truncated hNLRs have any biological roles.

Here, we describe the functional analysis of truncated hNLRs. To our surprise, NRG1C negatively regulated autoimmunity mediated by the *A. thaliana* TNL autoimmune mutant *chilling sensitive 3, 2D* (*chs3-2D*), playing an opposite role from its full-length paralogs NRG1A/1B. Plants overexpressing *NRG1C* phenocopied the *nrg1a nrg1b* double mutant and the *SENESCENCE-ASSOCIATED GENE 101* (*sag101*) single mutant. Biochemical analysis suggested that NRG1C might function by interfering with the ENHANCED DISEASE SUSCEPTIBILITY 1 (EDS1)–SAG101 complex. Interestingly, NRG1Cs from different Brassicaceae species are functionally exchangeable. In addition, the *N. benthamiana* truncated NRG2 also antagonizes NRG1-mediated cell death and bacterial growth restriction. In summary, our study uncovers an unexpected role of N-terminally truncated hNLRs, which likely evolved to balance the activities of their corresponding full-length hNLRs.

Results

NRG1C is evolutionarily conserved in Brassicaceae and its expression is highly induced in TNL-type autoimmune mutants and upon pathogen infection

BLASTp analysis revealed that NRG1C-type N-terminally truncated hNLRs are present in all eight sequenced Brassicaceae species and *N. benthamiana* (Figure 1, A and B, Supplemental Figure S1 and Supplemental Table S1). Additionally, *NRG1C* can be found in all examined *A. thaliana* accessions, arguing against it being a pseudogene. However, no NRG1C homolog was found in available protein databases of other land plants. Interestingly, like *A. thaliana NRG1C*, other Brassicaceae *NRG1C* homologs tend to cluster with the full-length *NRG1* genes in their genomes (Supplemental Table S1). Phylogenetic analysis indicated that all Brassicaceae NRG1Cs came from the same ancestor (Figure 1B). The Brassicaceae *NRG1C* genes likely originated from either an initial gene duplication of the *NRG1A/1B* ancestor and a subsequent N-terminal loss, or partial gene duplication. In contrast, NbNRG2 and NbNRG1 belong to a distinct clade from Brassicaceae NRG1, which is suggestive of a different evolutionary pathway between *N. benthamiana* NRG1s and Brassicaceae NRG1s (Figure 1B; Supplemental Figure S1). In *Brassica rapa*, there are two close *NRG1C* homologs found in two gene clusters. Brara.I00877.1 and Brara.G01211.1 share 75.4% and 62.0% amino acid identity, or 86.2% and 75.5% similarity with *A. thaliana* NRG1C, respectively (Supplemental Figure S1 and Supplemental Table S1). However, phylogenetic analysis indicated that Brara.G01211.1 might not be an NRG1C homolog, as it contains a full NB domain (Supplemental Figure S1) and is distinct from the NRG1C clade (Figure 1B).

DA1-RELATED PROTEIN 5 (DAR5, AT5G66630) was proposed to be a chimeric protein resulting from a translocation of NRG1C and a fusion with a member of the nearby cluster carrying DAR homologs, DAR7 (AT5G66610) to DAR3 (AT5G66640) (Meyers et al., 2003). Coincidently, DAR5 carries RPW8 CC, NB, and LIM (Lin11, Isl-1, and Mec-3) domains, but no LRRs. DAR5 shares high similarity with NRG1s in *A. thaliana* (Andolfo et al., 2019; Castel et al., 2019). However, DAR5 seems to be unique in *A. thaliana*, as BLAST searches failed to identify putative DAR5 homologs in the genomes of all other sequenced plant species.

To test whether the truncated *NRG1C* and *DAR5* are involved in TNL-mediated immunity, we measured their expression levels in TNL autoimmune mutants. *suppressor of npr1-1, constitutive 1* (*snc1*), and *chs3-2D* contain gain-of-function mutations in the *TNLs SNC1* and *CHS3*, respectively, resulting in TNL-mediated autoimmunity (Li et al., 2001; Bi et al., 2011). *NRG1C* transcripts were ~200- and 7,000-fold upregulated in *snc1* and *chs3-2D*, respectively, compared to Col-0 wild-type (WT) (Figure 1C). However, no significant changes in *DAR5* transcript levels were observed (Supplemental Figure S2A). Interestingly, both *NRG1C* and *DAR5* were upregulated in *A. thaliana* upon infection by the virulent bacterial pathogen *Pseudomonas syringae* pv. *tomato* (*P.s.t.*) DC3000, as revealed in an RNA-sequencing dataset (Howard et al., 2013). However, our qRT-PCR (quantitative Reverse Transcription-PCR) analysis indicated that the transcription of *NRG1C*, but not *DAR5*, was highly induced by *P.s.t.* DC3000 (Figure 1D; Supplemental Figure S2B). These expression analyses suggest that *NRG1C* in the *NRG1* gene cluster may play roles in biotic responses against pathogens.

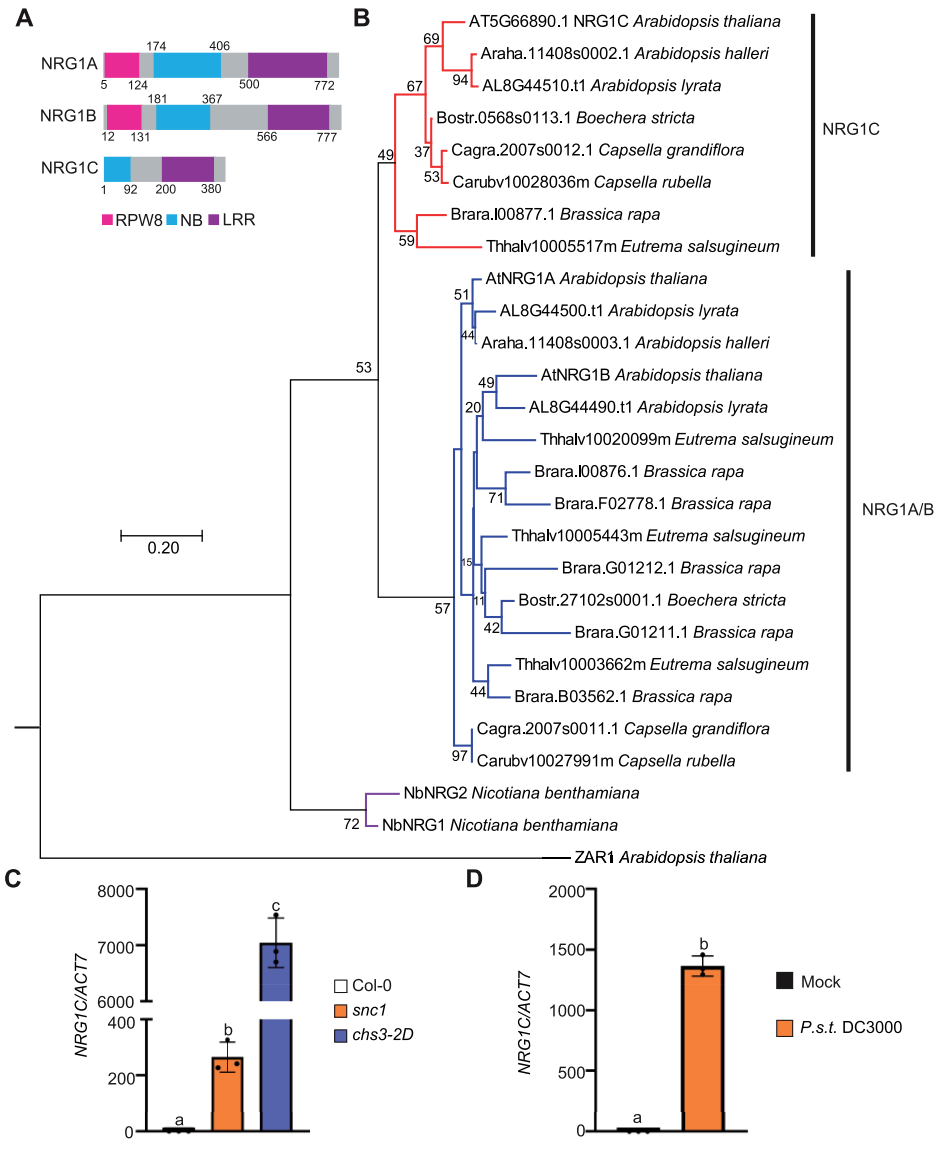

Figure 1 *NRG1C* is evolutionarily conserved in Brassicaceae, and its transcription is induced in TNL-type autoimmune mutants and upon pathogen infection. A, Protein domain diagrams of NRG1A, NRG1B, and NRG1C. Numbers represent amino acid positions relative to the translation start sites. NRG1C lacks the RPW8 CC and part of the NB domains. B, Phylogenetic tree of NRG1A/1B/1C homologs. Putative NRG1A/1B/1C homologs were obtained from Phytozome (Brassicaceae species) and Sol Genomics Network (*N. benthamiana*) using *A. thaliana* NRG1A and NRG1C protein sequences as respective queries. ZAR1 was used as an outgroup to root the tree. MUSCLE was used for sequence alignment, and the Neighbor-joining tree was generated using full-length NRG1C and homologous parts of all other corresponding NRG1 homologs with the JTT model and using 2000 bootstrap replicates in MEGA version 7.0. Numbers at the nodes indicate the bootstrap values as a percentage based on neighbor-joining analysis. C, *NRG1C* gene expression in 4-week-old soil-grown autoimmune mutants *snc1* and *chs3-2D*, as determined by qRT-PCR (Col-0 served as the WT control, and the transcript level in Col-0 was arbitrarily set at 1.0). Statistical significance is indicated by different letters ($P < 0.01$). Error bars represent means ± standard deviation (SD) ($n = 3$). Three independent experiments were carried out with similar results. D, qRT-PCR analysis of the expression of *NRG1C* upon *P.s.t.* DC3000 infection. Four-week-old soil-grown WT plants were inoculated with 10 mM $MgCl_2$ (Mock) or *P.s.t.* DC3000 (OD_{600} = 0.2). Samples were collected at 12 hpi. Values were normalized to the level of *ACTIN7*, and the transcript level in Mock treatment was set at 1.0. Error bars represent means ± SD ($n = 3$). Three independent experiments were carried out with similar results.

NRG1C, but not *DAR5*, negatively regulates *chs3-2D*- and *snc1*-mediated autoimmunity

We first used an overexpression approach to examine the role of these truncated NLRs. *NRG1C* and *DAR5* were individually overexpressed in the *chs3-2D* and *snc1* backgrounds. To our surprise, overexpression of *NRG1C* fully suppressed *chs3-2D*-mediated dwarfism (Figure 2, A–C) and enhanced disease resistance to the oomycete pathogen *Hyaloperonospora arabidopsidis* (*H.a.*) Noco2 (Figure 2D), with no reduction in *NRG1A/1B* transcript levels (Figure 2E). In contrast, no

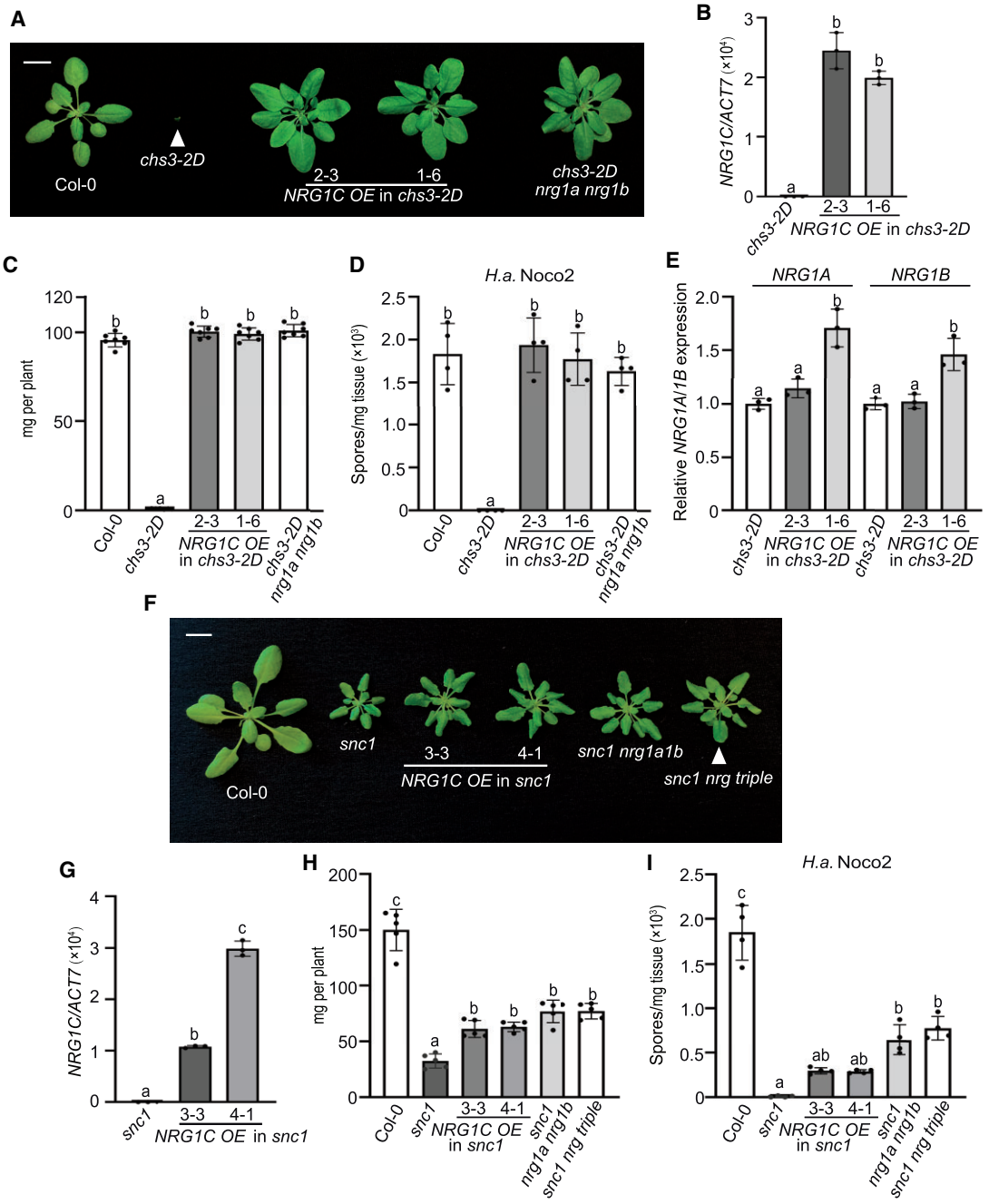

Figure 2 *NRG1C* negatively regulates *chs3-2D* and *snc1*-mediated autoimmunity. A, Morphology of 4-week-old soil-grown plants of Col-0, *chs3-2D*, two independent transgenic lines of *NRG1C OE* in the *chs3-2D* background and *chs3-2D nrg1a nrg1b*. Bar = 1 cm. B, *NRG1C* gene expression in the indicated 2-week-old plate-grown plants, as determined by qRT-PCR (*chs3-2D* served as a control whose *NRG1C* transcript level was set at 1.0). Statistical significance is indicated by different letters ($P < 0.01$). Error bars represent means ± SD ($n = 3$). Two independent experiments were carried out with similar results. C, Fresh weights of the plants in (A). Statistical significance is indicated by different letters ($P < 0.01$). Error bars represent means ± SD ($n = 7$). D, Quantification of *H.a.* Noco2 sporulation in the indicated genotypes 7 days post-inoculation (dpi) with 10^5 spores per ml water. Statistical significance is indicated by different letters ($P < 0.01$). Error bars represent means ± SD ($n = 4$). Three independent experiments were carried out with similar results. E, *NRG1A/1B* gene expression in the indicated 4-week-old soil-grown plants, as determined by qRT-PCR (*chs3-2D* served as a control whose *NRG1A/1B* transcript level was set at 1.0). Statistical significance is indicated by different letters ($P < 0.01$). Error bars represent means ± SD ($n = 3$). Three independent experiments were carried out with similar results. F, Morphology of 4-week-old soil-grown plants of Col-0, *snc1*, two independent transgenic lines of *NRG1C OE* in the *snc1* background, *snc1 nrg1a nrg1b* and *snc1 nrg triple*. Bar = 1 cm. G, *NRG1C* gene expression in the indicated 2-week-old plate-grown plants, as determined by qRT-PCR (*snc1* served as a control whose *NRG1C* transcript level was set at 1.0). Statistical significance is indicated by different letters ($P < 0.01$). Error bars represent means ± SD ($n = 3$). Two independent experiments were carried out with similar results. H, Fresh weights of the plants in (F). Statistical significance is indicated by different letters ($P < 0.01$). Error bars represent means ± SD ($n = 5$). I, Quantification of *H.a.* Noco2 sporulation in the indicated genotypes at 7 dpi with 10^5 spores per ml water. Statistical significance is indicated by different letters ($P < 0.01$). Error bars represent means ± SD ($n = 4$). Three independent experiments were carried out with similar results.

suppression of *chs3-2D*-mediated growth defects was observed upon *DAR5* overexpression (Supplemental Figure S2, C and D). Furthermore, overexpressing *NRG1C* partially suppressed *snc1*-mediated dwarfism to a level similar to that of the *nrg1a/1b* and *nrg1a/1b/1c* deletion mutants (Wu et al., 2019) (Figure 2, F–H). Consistently, the enhanced disease resistance to *H.a.* Noco2 (Figure 2I) in *snc1* was partially suppressed upon *NRG1C* overexpression. However, the *snc1 DAR5 OE* lines did not show significant differences in growth compared with *snc1* (Supplemental Figure S2, E and F). Taken together, these results indicate that NRG1C negatively regulates *chs3-2D* and *snc1*-mediated autoimmunity to different degrees. Intriguingly, these *NRG1C* overexpression phenotypes closely resemble those of the *nrg1a nrg1b* double mutant and the *sag101* single mutant (Xu et al., 2015; Wu et al., 2019).

ADR1-L3 is dispensable for *snc1*-mediated autoimmunity and RPP4-mediated immunity

Similar to NRG1C in the NRG1 family, the *A. thaliana* ADR1 hNLR family includes a truncated ADR1-L3, missing the N-terminal RPW8 domain (Supplemental Figure S3). In contrast to the broad presence of NRG1C in Brassicaceae, an ADR1-L3 homolog is only found in Drummond's rockcress (*Boechera stricta*; Supplemental Figure S3). To test whether ADR1-L3 is involved in immunity conferred by ADR1-dependent sNLRs, we overexpressed *ADR1-L3* in the *snc1* background. However, *snc1*-mediated growth defects (Supplemental Figure S4A) and enhanced disease resistance (Supplemental Figure S4C) were not altered upon *ADR1-L3* overexpression (Supplemental Figure S4B). Furthermore, *ADR1-L3* overexpression lines in the WT background were not susceptible to the oomycete pathogen *H.a.* Emwa1 (Supplemental Figure S4, D and E), which is recognized by the ADR1-dependent TNL RECOGNITION OF PERONOSPORA PARASITICA 4 (RPP4) (Bonardi et al., 2011; Dong et al., 2016). Taken together, unlike NRG1C, ADR1-L3 does not seem to play any roles in TNL-mediated autoimmunity and defense.

Overexpression of *NRG1C* has no effect on *chs1-2*- and *chs2-1*-mediated autoimmunity, RPS2 and RPS4-mediated immunity, or basal defense

To further test the specificity of NRG1C, we overexpressed *NRG1C* in additional autoimmune mutants. In *chilling sensitive 1, 2* (*chs1-2*), a missense mutation in a truncated TN protein (Wang et al., 2013) results in constitutive cell death and defense responses at low temperatures (Zbierzak et al., 2013). The chilling sensitive mutant *chs2-1* contains a gain-of-function mutation in the TNL *RPP4* (Huang et al., 2010). However, neither *chs1-2* nor *chs2-1*-mediated temperature-dependent autoimmunity was suppressed upon *NRG1C* overexpression (Supplemental Figure S5, A–D). Consistently, the oomycete pathogen *H.a.* Emwa1 failed to grow in *NRG1C OE* lines in the WT background (Supplemental Figure S5, E–G).

We also challenged two independent *NRG1C OE* lines (in the WT Col-0 background) with *P.s.t.* DC3000 expressing either AvrRps4 or AvrRpt2 effectors, which are recognized by TNL RESISTANT TO *P. SYRINGAE* 4 (RPS4) or CNL RPS2, respectively. However, no altered disease resistance against these avirulent pathogens was detected (Supplemental Figure S6, A and B). When challenged with *P.s.t.* DC3000, the *NRG1C OE* lines exhibited similar bacterial growth as WT, suggesting that overexpression of *NRG1C* does not compromise the basal defense response either (Supplemental Figure S6C). Therefore, NRG1C seems to function specifically in TNL-mediated immune responses, with different strengths for distinct TNLs. The differential contributions of NRG1C to TNL signaling are reminiscent of the phenotypes of *nrg1a nrg1b* or *sag101* knockout mutants, which show major effects in *chs3-2D* but relatively mild suppression in *snc1* and no effects in *chs1-2*, *chs2-1*, RPS4, or RPS2-mediated autoimmunity or bacterial growth restriction (Feys et al., 2005; Xu et al., 2015; Castel et al., 2019; Wu et al., 2019).

NRG1C is required for HopQ1-1-triggered defense

NbNRG1 is essential for immune signaling triggered by the effector HopQ1-1 (Qi et al., 2018). To test whether *A. thaliana* NRG1s play roles in effector HopQ1-1-triggered defense responses, we performed bacterial infection experiments using the *nrg1a nrg1b* double mutant and *NRG1C OE* lines. As *P.s.t.* DC3000 carries diverse effectors that can mask the effects of HopQ1-1, *P.s.t.* DC3000 D36E, in which all 36 T3SS (Type III secretion system) effector genes and coronatine biosynthesis genes were deleted, was used as a background to avoid interference from other effectors (Wei et al., 2015). As shown in Figure 3A, WT plants inoculated with *P.s.t.* DC3000 D36E expressing HopQ1-1 showed induced *NRG1C* expression, suggesting a potential role for NRG1C in HopQ1-1-triggered defense responses. Additionally, less *P.s.t.* DC3000 D36E HopQ1-1 bacterial growth was detected in WT plants compared to *P.s.t.* DC3000 D36E (Supplemental Figure S6D), indicating that there is likely a yet-to-be identified *A. thaliana* R protein that can respond to the effector HopQ1-1. Indeed, *NRG1C OE* lines exhibited enhanced disease susceptibility to *P.s.t.* DC3000 D36E HopQ1-1 to a level similar to that of the *nrg1a nrg1b* double mutant and *sag101* single mutant (Figure 3B). In contrast, no bacterial growth difference was observed among the *NRG1C OE* lines, *nrg1a nrg1b*, or *sag101-1* compared with WT when challenged with *P.s.t.* DC3000 D36E (Supplemental Figure S6E). Taken together, these data indicate that NRG1C antagonizes HopQ1-1-triggered NRG1-dependent defense responses in *A. thaliana*. The phenotypes of the *NRG1C* overexpression plants seem identical to those of the *nrg1a nrg1b* double mutant and the *sag101* single mutant.

NRG1C antagonizes the AvrRPS4-mediated HR

AvrRPS4 can activate RESISTANT TO RALSTONIA SOLANACEARUM 1 (RRS1)/RPS4 pairs, resulting in HR in the Col-0 background (Saucet et al., 2015). This HR was compromised in the Col-0 *nrg1a nrg1b* double mutant, although no difference in *P.s.t.* AvrRPS4 bacterial growth was observed (Supplemental Figure S6A) (Castel et al., 2019;

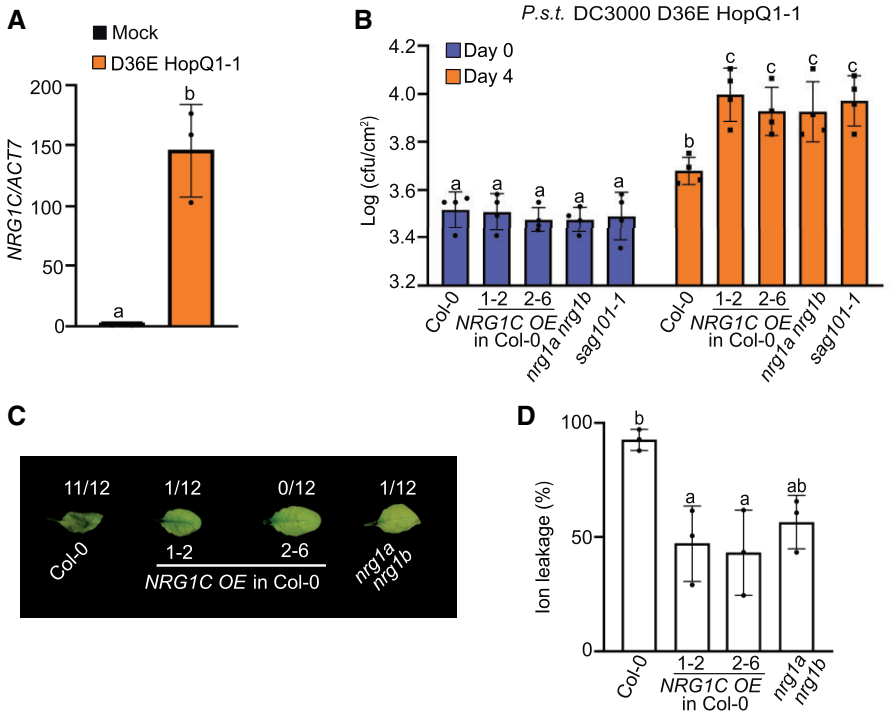

Figure 3 NRG1C antagonizes HopQ1-1-mediated bacterial growth and AvrRPS4-mediated HR. A, qRT-PCR analysis of the expression of *NRG1C* upon *P.s.t.* DC3000 D36E HopQ1-1 infection. 4-week-old soil-grown Col-0 plants were inoculated with 10 mM $MgCl_2$ (Mock) or *P.s.t.* DC3000 D36E HopQ1-1 (OD_{600} = 0.2). Samples were collected at 12 hpi. Values were normalized to the level of *ACTIN7*, and the transcript level in Mock treatment was set at 1.0. Error bars represent means ± SD (n = 3). Three independent experiments were carried out with similar results. B, Growth of *P.s.t.* DC3000 D36E HopQ1-1 in 4-week-old leaves of the indicated genotypes at 0 and 4 dpi with bacterial inoculum of OD_{600} = 0.001. Statistical significance is indicated by different letters ($P < 0.05$). Error bars represent means ± SD (n = 4). Three independent experiments were carried out with similar results. C, HR in leaves infiltrated with *Pf0-1* AvrRPS4. 4-week-old *A. thaliana* leaves of the indicated genotypes were infiltrated with *Pf0-1* expressing AvrRPS4 at OD_{600} = 0.2. Photographs were taken at 36 hpi. The numbers indicate the number of plants displaying HR out of the total number of plants tested. Three independent experiments were carried out with similar results. D, Ion leakage of *A. thaliana* leaves upon *Pf0-1*_AvrRPS4 infiltration under the same conditions as for C. Twelve infiltrated leaves were collected as one biological replicate. Individual dots indicate different biological replicates. Error bars represent means ± SD (n = 3). Statistical significance is indicated by different letters ($P < 0.01$). Three independent experiments were carried out with similar results.

Lapin et al., 2019). *NRG1C* was significantly upregulated at 6 and 12 h post-inoculation (hpi) with *P.s.t* DC3000 AvrRPS4, but not at 1 hpi (Howard et al., 2013), suggesting that NRG1C plays roles in AvrRPS4-triggered immunity. We thus tested whether NRG1C regulates the RRS1/RPS4-mediated HR. The effector AvrRPS4 was delivered using the *Pseudomonas fluorescens* strain *Pf0-1* containing the type III secretion system (*Pf0-1* EtHAn), but lacking type III effector genes (Thomas et al., 2009). Similar with the phenotype of the *nrg1a nrg1b* double mutant (Castel et al., 2019; Lapin et al., 2019), RRS1/RPS4-mediated HR was lost in *NRG1C OE* lines (Figure 3, C and D). The striking overall phenotypic resemblance between *NRG1C OE* lines and the *nrg1a nrg1b* double mutant suggests that NRG1C may function antagonistically with NRG1A/1B to regulate defense responses.

NRG1C antagonizes the NRG1–SAG101 module, in parallel with the ADR1-PAD4 module

The similar phenotypes of *adr1 triple* and *phytoalexin deficient 4* (*pad4*) mutants (Dong et al., 2016), and the additive effects between SAG101 and PAD4 (Rietz et al., 2011) or NRG1s and ADR1s (Lapin et al., 2019; Wu et al., 2019; Saile et al., 2020), allude to an EDS1–ADR1–PAD4 signaling module that works in parallel with the EDS1–NRG1–SAG101 module to regulate downstream events in TNL immunity. The existence of the EDS1–PAD4–ADR1 and EDS1–SAG101–NRG1 complexes corroborates the two independent genetic modules (Sun et al., 2021; Wu et al., 2021). To examine the contribution of NRG1C in these modules, we generated higher-order mutants combining loss-of-function mutations from different complexes in the *snc1* background. The dwarfism and increased *PATHOGENESIS-RELATED 1* (*PR1*) gene expression of *snc1* were partially suppressed by introducing mutations in *SAG101* (Feys et al., 2005) or the *NRG1* cluster (Wu et al., 2019) (Figure 4, A and B). However, the *snc1 sag101-1 nrg triple* mutants resembled the *snc1 sag101-1* and *snc1 nrg triple* mutants in terms of morphology (Figure 4A) and *PR1* gene expression levels (Figure 4B), confirming the notion that SAG101 functions in the same pathway as NRG1A/1B. By contrast, the increased *PR1* gene expression of *snc1* was largely, but not

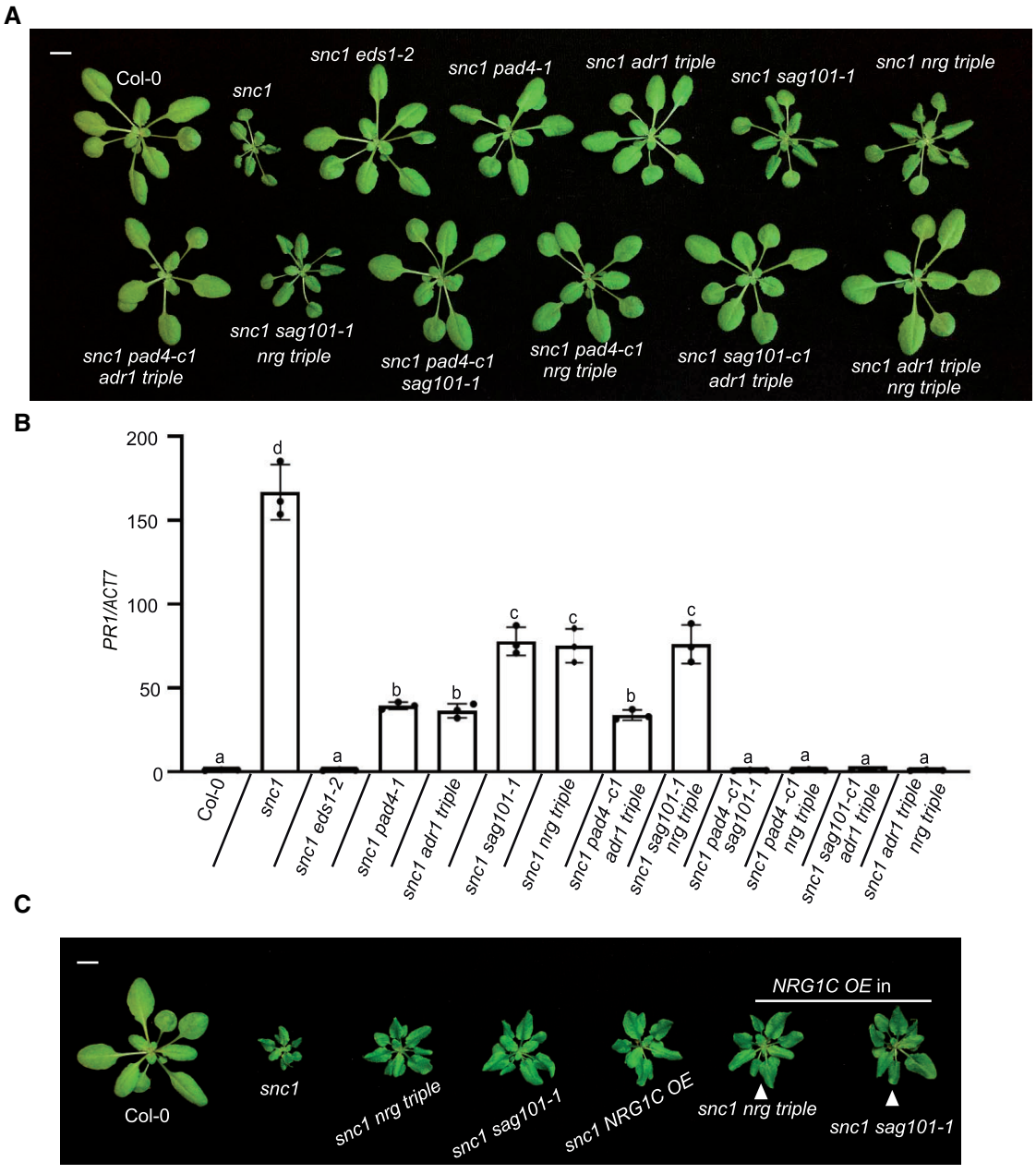

Figure 4 NRG1C antagonizes the EDS1–NRG1–SAG101 module, which functions in parallel with the EDS1–ADR1–PAD4 module. A, Morphology of 4-week-old soil-grown plants of Col-0, *snc1*, *snc1 eds1-2*, *snc1 pad4-1*, *snc1 adr1 triple*, *snc1 sag101-1*, *snc1 nrg triple*, *snc1 pad4-c1 adr1 triple*, *snc1 sag101-1 nrg triple*, *snc1 pad4-c1 sag101-1*, *snc1 pad4-c1 nrg triple*, *snc1 sag101-c1 adr1 triple* and *snc1 adr1 triple nrg triple*. *pad4-c1*, and *sag101-c1* alleles were generated using CRISPR–Cas9-mediated genome editing. Bar = 1 cm. B, *PR1* gene expression in the indicated 4-week-old soil-grown plants, as determined by qRT-PCR (Col-0 served as a control whose *PR1* transcript level was set at 1.0). Statistical significance is indicated by different letters ($P < 0.01$). Error bars represent means ± SD ($n = 3$). Three independent experiments were carried out with similar results. C, Morphology of 4-week-old soil-grown plants of Col-0, *snc1*, *snc1 nrg triple*, *snc1 sag101-1*, *snc1 NRG1C* OE, *snc1 nrg triple NRG1C OE*, and *snc1 sag101-1 NRG1C OE*. Bar = 1 cm.

fully, suppressed by *adr1 triple* or *pad4-1* (Figure 4B), although the sizes of *snc1 adr1 triple* and *snc1 pad4-1* plants were WT like (Cheng et al., 2011; Dong et al., 2016) (Figure 4A). However, combining *adr1 triple* and *pad4* mutations together did not further reduce *PR1* gene expression (Figure 4B; Supplemental Figure S7), confirming the notion that ADR1s and PAD4 work in the same pathway. In contrast, mutants containing mutations in two components from different modules, including *snc1 pad4-c1 sag101-1*, *snc1 pad4-c1 nrg triple*, *snc1 sag101-c1 adr1 triple*, and *snc1 adr1 triple nrg triple*, exhibited fully restored WT-like levels of *PR1* expression (Figure 4, A and B; Supplemental Figure S7). Taken together, these epistasis analyses data further confirm the notion that two distinct modules are present in TNL pathways that act in parallel: one includes PAD4–ADR1s and the other includes SAG101–NRG1A/1B.

To examine the relationship between NRG1C and the two distinct modules, we overexpressed *NRG1C* in the *snc1 nrg triple*, *snc1 sag101-1*, *snc1 pad4-1*, or *snc1 adr1 triple* backgrounds. As shown in Figure 4C, the dwarfism of *snc1 nrg triple* and *snc1 sag101-1* was not further suppressed by *NRG1C* overexpression. In agreement with this finding, *snc1 sag101-1 NRG1C OE* and *snc1 nrg triple NRG1C OE* resembled the *snc1 sag101-1* and *snc1 nrg triple* mutants in terms of *PR1* gene expression (Supplemental Figure S8A). Specifically, the increased *PR1* gene expression in *snc1* was reduced by either *nrg triple* or *sag101*, but was not further reduced by *NRG1C* overexpression (Supplemental Figure S8A). In contrast, the partial suppression of upregulated *PR1* gene expression in *snc1* by *adr1 triple* or *pad4-1* was further suppressed to WT levels when *NRG1C* was overexpressed in the *snc1 adr1 triple* or *snc1 pad4-1* background (Supplemental Figure S8B). These comprehensive epistasis analyses support the notion that NRG1C indeed specifically antagonizes the SAG101-NRG1A/1B module.

Loss of *NRG1C* enhances resistance mediated by some TNLs

As plants overexpressing *NRG1C* exhibited defects in TNL-mediated defense responses, we further examined the phenotypes of *nrg1c* knockout mutants. A T-DNA insertion mutant (*nrg1c-1*, Sail_1265_F08) of *NRG1C* (Wu et al., 2019) and two independent deletion alleles generated by CRISPR (Clustered Regularly Interspaced Short Palindromic Repeats)/Cas9 (CRISPR-associated protein 9)-mediated genome editing (Supplemental Figure S7) were used to analyze the knockout phenotypes of *nrg1c*. Morphologically, these mutant alleles were completely WT-like. When they were challenged with *P.s.t.* DC3000 D36E HopQ1-1 (Figure 5A), all three *nrg1c* mutants exhibited enhanced resistance to *P.s.t.* DC3000 D36E HopQ1-1. However, no altered growth of *P.s.t.* DC3000 D36E was detected (Figure 5B), which is suggestive of a specific negative role of NRG1C in HopQ1-1-triggered defense responses. Interestingly, under a short-day regime (8-h light/16-h dark), the dwarfism of *snc1* was further enhanced when *NRG1C* was knocked out (Figure 5, C and D). This enhancement was not observed previously when these plants were grown under long-day conditions (16-h light/8-h dark) (Wu et al., 2019). Consistently, increased *PR1* gene expression was observed in the *snc1 nrg1c* double mutants (Figure 5E). In parallel, *PR1* gene expression was also upregulated in the *chs3-2D nrg1c* double mutants compared to their parent *chs3-2D* (Figure 5F). These data indicate that the loss of *NRG1C* enhances the defense responses of these two autoimmune mutants. In conclusion, NRG1C plays a negative role in immune regulation and its loss leads to enhanced immunity in autoimmune backgrounds and against *P.s.t.* DC3000 D36E HopQ1-1.

NRG1C does not affect *NRG1A/1B* by transcriptional interference

As *NRG1C* encodes a truncated hNLR that antagonizes the SAG101–NRG1A/1B module, we reasoned that it might interfere with *NRG1A/1B* transcription via RNA-mediated interference due to their sequence similarity. To test this, we overexpressed *NRG1C* with a premature stop codon at position 213 of the predicted *NRG1C* mRNA sequence in the *chs3-2D* background. Such a mutation would yield a non-functional protein ($NRG1C^{T71^*}$) but a normal transcript. No alterations in *chs3-2D*-mediated dwarfism (Figure 6, A and B) or enhanced disease resistance to *H.a.* Noco2 (Figure 6C) were observed upon overexpression of $NRG1C^{T71^*}$ (Supplemental Figure S9A). Additionally, no reduction in *NRG1A/1B* transcript levels was detected upon *NRG1C* overexpression in either the *chs3-2D* or WT background (Supplemental Figure S9, B; Figure 2, E). Taken together, these data suggest that NRG1C does not affect mRNA levels of the full-length helper *NRG1A/1B*. Thus, if NRG1C interferes with NRG1A/1B, the effects are likely at the protein level.

NRG1C antagonizes NRG1A D485V-mediated autoimmunity in *A. thaliana* and NRG1A D485V-mediated HR in *N. benthamiana*

To further examine the hypothesis that NRG1C directly interferes with NRG1A/1B, we overexpressed *NRG1C* in transgenic plants expressing *NRG1A D485V*, an auto-active version of NRG1A that constitutively activates immunity (Wu et al., 2019). The dwarfism and enhanced resistance of *NRG1A D485V* were largely suppressed upon *NRG1C* overexpression (Figure 6, D–F and Supplemental Figure S9, C), while no reduction in *NRG1A* transcript or protein levels was observed (Supplemental Figure S9, D and E). These results further support the notion that the negative regulation of NRG1A by NRG1C does not function through transcriptional or post-transcriptional repression. In contrast, overexpression of *NRG1C* did not alter the autoimmunity of *ADR1-L2 D484V*, an auto-active variant of ADR1-L2 (Roberts et al., 2013) (Supplemental Figure S10, A–D).

Consistent with our observation in *A. thaliana*, NRG1A D485V-triggered HR in *N. benthamiana* was alleviated when NRG1C was expressed in these leaves (Supplemental Figure S10, E and F), although the same amount of NRG1A D485V protein accumulated (Supplemental Figure S10G). Taken together, these data indicate that NRG1A-mediated autoimmunity and HR are negatively regulated by NRG1C and that the effects of NRG1C seem to be specific to NRG1-type hNLR-mediated defense responses.

NRG1C does not associate with full-length NRG1A

Since NRG1C does not affect the mRNA or protein levels of full-length NRG1A (Supplemental Figure S9), another hypothesis is that NRG1C interferes with NRG1A/1B through protein-protein interactions. We combined TurboID-based

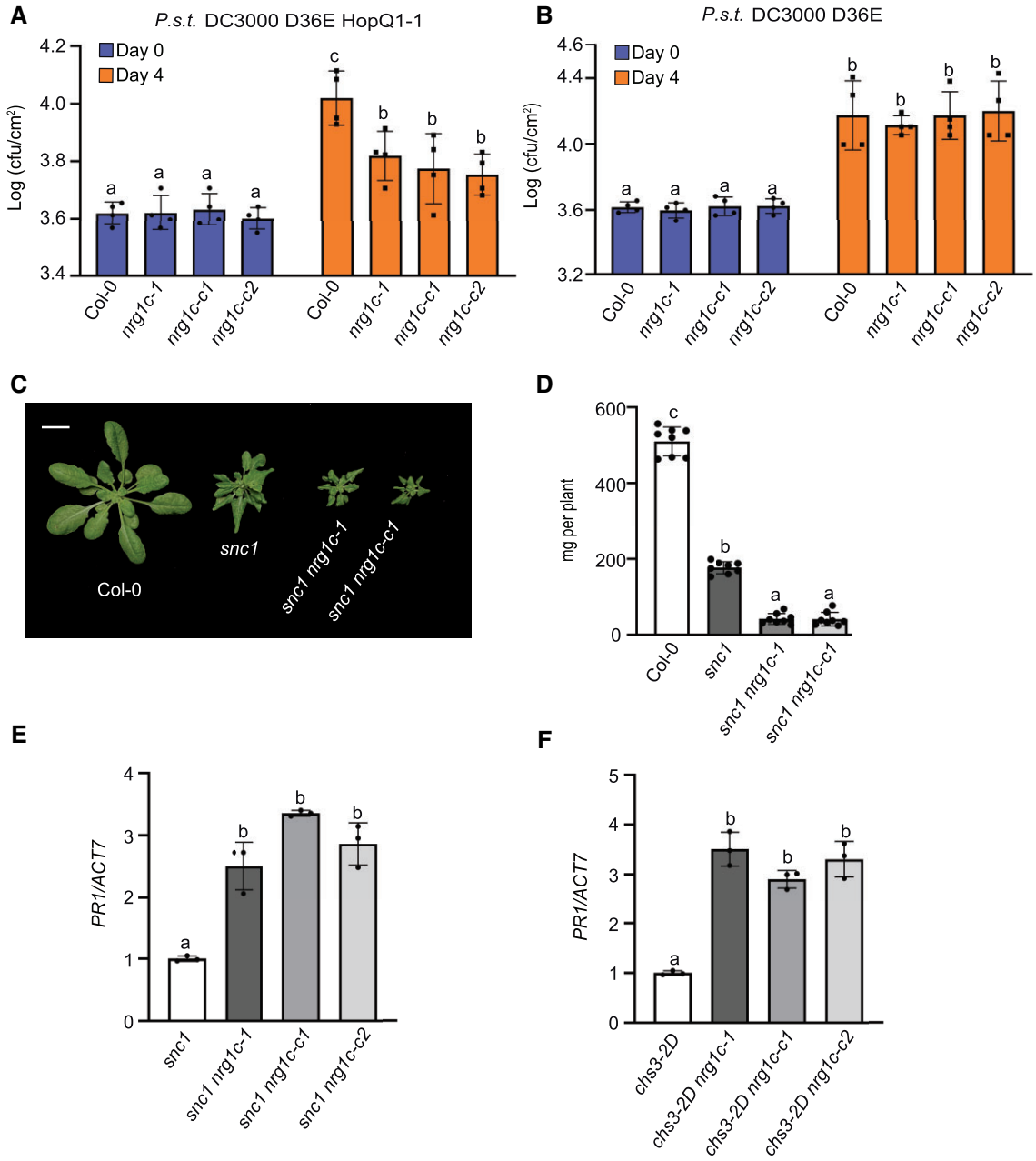

Figure 5 Loss of *NRG1C* enhances TNL-mediated defense responses. A and B, Growth of *P.s.t.* DC3000 D36E HopQ1-1 (A) or *P.s.t.* DC3000 D36E (B) in 4-week-old leaves of the indicated genotypes at 0 and 4 dpi with bacterial inoculum of OD_{600} = 0.001. Statistical significance is indicated by different letters ($P < 0.05$). Error bars represent means ± SD ($n = 4$). Three independent experiments were carried out with similar results. C, Morphology of 6-week-old soil-grown plants of Col-0, *snc1*, *snc1 nrg1c-1*, and *snc1 nrg1c-c1* under short-day conditions (8-h light/16-h dark). Bar = 1 cm. D, Fresh weights of the plants in (C). Statistical significance is indicated by different letters ($P < 0.01$). Error bars represent means ± SD ($n = 8$). E and F, *PR1* gene expression in the indicated 2-week-old plate-grown plants, as determined by qRT-PCR (*snc1* (E) and *chs3-2D* (F) served as controls whose *PR1* transcript level was set at 1.0). Statistical significance is indicated by different letters ($P < 0.01$). Error bars represent means ± SD ($n = 3$). Three independent experiments were carried out with similar results.

proximity labeling and co-immunoprecipitation (IP) to allow detection of transient protein–protein interactions with low-abundance proteins (Zhang et al., 2019; Wu et al., 2020). As shown in Supplemental Figure S11A, expressing NRG1A-HA-TurboID partially restored the morphological suppression of *chs3-2D nrg1a nrg1b*, suggesting that the fusion protein is functional. However, when NRG1A-HA-TurboID was co-expressed with NRG1C-3FLAG, NRG1C-3FLAG failed to pull down or be biotinylated by NRG1A-HA-TurboID (Supplemental Figure S11B). This negative interaction result suggests that the NRG1C-mediated negative regulation of NRG1A-mediated defense responses does not function via direct protein interference. However, we cannot exclude the possibility that the *in planta* interactions between the two proteins could not be detected due to complex conformation constraints.

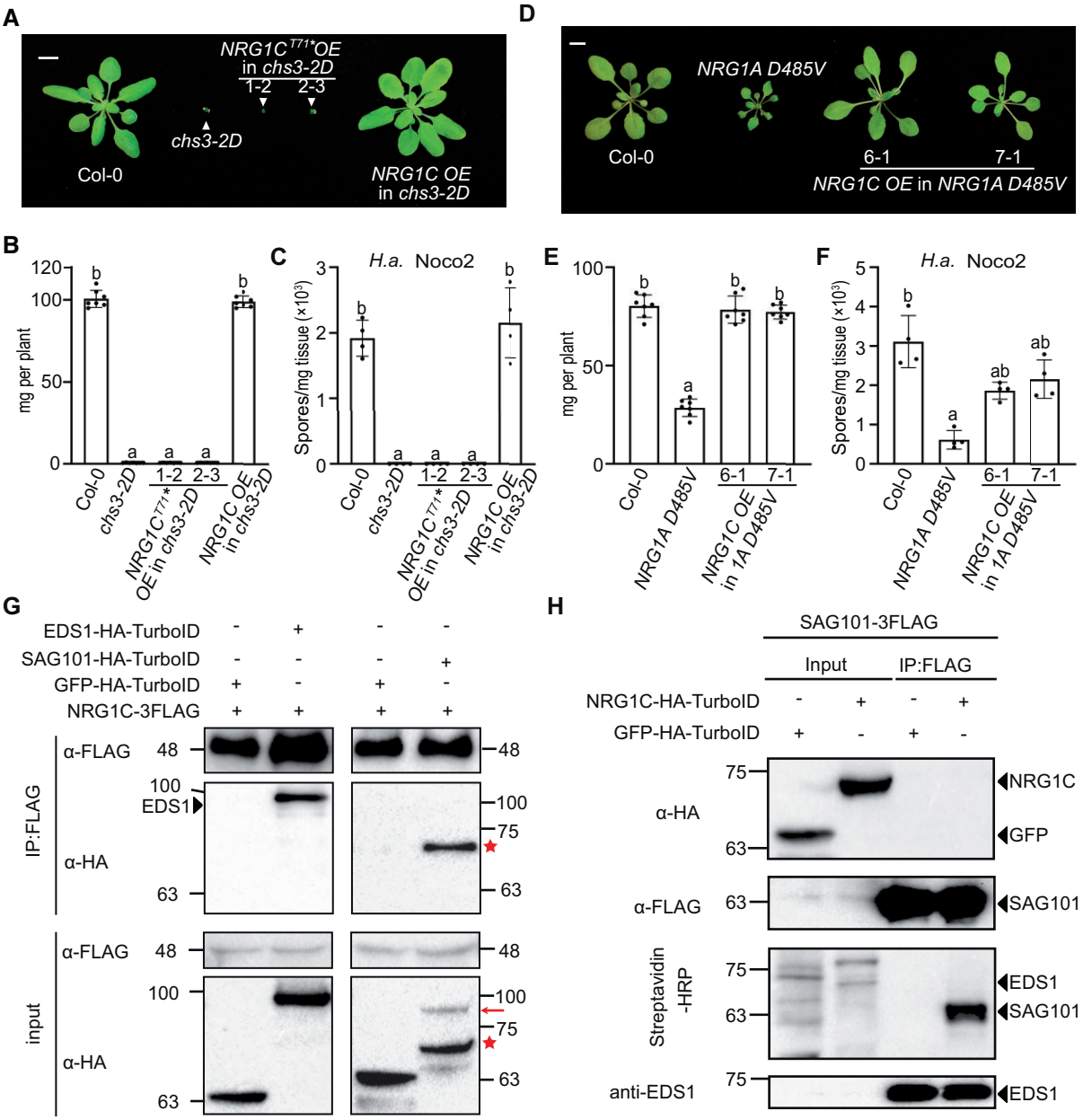

Figure 6 NRG1C negatively regulates NRG1A/1B-dependent defense responses via its association with the EDS1–SAG101 complex, but not by transcriptional interference of *NRG1A/1B*. A, Morphology of 4-week-old soil-grown plants of Col-0, *chs3-2D*, two independent transgenic lines of *NRG1C*^{T71*} *OE* in the *chs3-2D* background and *NRG1C OE* in the *chs3-2D* background. *NRG1C*^{T71*} carries an early stop codon to disrupt protein synthesis, but not transcription. Bar = 1 cm. B and E, Fresh weights of the plants in (A) or (D). Statistical significance is indicated by different letters ($P < 0.01$). Error bars represent means ± SD ($n = 7$). C and F, Quantification of *H.a.* Noco2 sporulation in the indicated genotypes at 7 dpi with 10^5 spores per milliliter water. Statistical significance is indicated by different letters ($P < 0.01$). Error bars represent means ± SD ($n = 4$). Three independent experiments were carried out with similar results. D, Morphology of 3-week-old soil-grown plants of Col-0, *NRG1A D485V*, and two independent transgenic lines of *NRG1C OE* in the *NRG1A D485V* background. *NRG1A D485V* was tagged with three FLAG epitopes in frame at its C-terminus. Bar = 1 cm. G, Co-IP of NRG1C-3FLAG with EDS1-HA-TurboID or SAG101-HA-TurboID in *N. benthamiana*. GFP-HA-TurboID served as a negative control. IP was carried out with anti-FLAG beads. The 3FLAG-tagged proteins were detected using an anti-FLAG antibody. The HA-tagged proteins were detected using an anti-HA antibody. The red arrow denotes SAG101-HA-TurboID, while the stars indicate unknown degradation products from SAG101-HA-TurboID. Three or two independent experiments were carried out with similar results to test the association between NRG1C and EDS1 or SAG101, respectively. H, Co-IP and biotinylation of SAG101-3FLAG with NRG1C-HA-TurboID in WT *A. thaliana* plants stably transformed with the two transgenes. IP was carried out with anti-FLAG beads. The 3FLAG-tagged proteins were detected using an anti-FLAG antibody. The HA-TurboID-tagged proteins were detected using an anti-HA antibody. EDS1 was detected using an anti-EDS1 antibody (Feys et al., 2001). The biotinylated proteins were detected using Streptavidin-HRP. Molecular mass markers in kiloDaltons are indicated on the left. Three independent experiments were carried out with similar results.

NRG1C associates with the EDS1–SAG101 complex

As plants overexpressing *NRG1C* also shared similar phenotypes with the *sag101* knockout mutants, and full-length NRG1A can form a complex with EDS1–SAG101 dimers (Sun et al., 2021), it is also possible that NRG1C attenuates NRG1A-mediated defense by interfering with SAG101 or EDS1. In support of this hypothesis, a near 73-fold more enrichment of NRG1C peptides was detected in *A. thaliana* SAG101-YFP IP-MS (mass spectrometry) analysis compared to full-length NRG1A (Sun et al., 2021). To further verify this observed NRG1C–SAG101 association, we co-infiltrated *N. benthamiana* leaves with *Agrobacterium* expressing NRG1C-3FLAG with EDS1-HA-TurboID, SAG101-HA-TurboID, or GFP-HA-TurboID. As shown in Figure 6G, NRG1C-3FLAG was able to pull-down EDS1-HA-TurboID and a degradation product of SAG101-HA-TurboID, but not the negative control GFP-HA-TurboID, although neither EDS1-HA-TurboID nor SAG101-HA-TurboID biotinylated NRG1C-3FLAG (Supplemental Figure S12, A and B). Therefore, NRG1C seems to work together with the EDS1–SAG101 dimers in a complex. The lack of biotinylation observed here is likely due to spatial constraints of the complex.

We further examined such interaction with a reciprocal assay using *A. thaliana* stable transgenic lines carrying both *NRG1C-HA-TurboID* and *SAG101-3FLAG*. Overexpression of *NRG1C-HA-TurboID* fully suppressed *chs3-2D*-mediated dwarfism (Supplemental Figure S11C), indicating that the fusion protein was functional. As shown in Figure 6H, although NRG1C-HA-TurboID was not observed in the SAG101-3FLAG pull-down, likely due to its low protein abundance or instability, NRG1C-HA-TurboID successfully biotinylated SAG101-3FLAG, but not EDS1, even though a large amount of EDS1 protein was pulled down. This suggests that SAG101 was in close proximity with the C-terminus of NRG1C, where TurboID was fused. The lack of EDS1 biotinylation by NRG1C could be due to constraints in space in the complex. However, neither EDS1 (Supplemental Figure S13, A and B) nor SAG101 (Supplemental Figure S13, C and D) protein levels were altered by *NRG1C* overexpression, confirming the notion that NRG1C does not affect the protein abundance of the EDS1–SAG101–NRG1A/1B complex.

Overexpression of the *B. rapa NRG1C* homolog suppresses *chs3-2D*-mediated defense

As *NRG1C*-type N-terminally truncated hNLRs appear to be conserved in Brassicaceae (Figure 1B), we further tested whether they are functionally exchangeable among different Brassicaceae species. To test this, we overexpressed *Brara.I00877.1* (*BraNRG1C*) in the *chs3-2D* mutant. Consistent with the finding (from phylogenetic analysis) that the Brassicaceae NRG1C family arose from a common ancestor (Figure 1B), overexpression of *BraNRG1C* fully rescued the *chs3-2D*-mediated dwarfism (Figure 7, A–C) and enhanced disease resistance to *H.a.* Noco2 (Figure 7D). Taken together, these results indicate that the NRG1C function is conserved in Brassicaceae species.

NbNRG2 negatively regulates HopQ1-1-mediated immunity in *N. benthamiana*

To further explore the function of truncated NRG1C outside the Brassicaceae, we examined the role of *N. benthamiana* NRG2 (NbNRG2) in HopQ1-1-triggered NRG1-dependent resistance (Schultink et al., 2017; Qi et al., 2018). When WT *N. benthamiana* leaves were challenged with *P.s.t.* DC3000 D36E HopQ1-1, more *NbNRG2* transcripts were detected (Supplemental Figure S14A), suggesting that NbNRG2 might play roles in HopQ1-1-trigerred defense responses. In addition, inoculation with *P.s.t.* DC3000 D36E HopQ1-1, but not *P.s.t.* DC3000 D36E, resulted in visible cell death in WT *N. benthamiana* (Supplemental Figure S14, B and C). In contrast, the cell death caused by *P.s.t.* DC3000 D36E HopQ1-1 was suppressed in the *N. benthamiana nrg1-1* mutant (Supplemental Figure S14C), in agreement with the previous finding that HopQ1-1-triggered defense responses are NRG1-dependent (Qi et al., 2018).

To test the function of NbNRG2 in *N. benthamiana*, we infiltrated leaves with *Agrobacteria* carrying *NbNRG2* or empty vector (EV) for 48 h and delivered the HopQ1-1 effector into the leaves via *P.s.t.* DC3000 D36E or *Agrobacteria* (Supplemental Figure S14D). Interestingly, overexpression of *NbNRG2* suppressed HopQ1-1-mediated HR, which was introduced by either *P.s.t.* DC3000 D36E HopQ1-1 (Figure 7, E–G) or *Agrobacteria* (Figure 7, H–J). Consistently, more *P.s.t.* DC3000 D36E HopQ1-1 bacterial growth was detected in *NbNRG2*-expressing leaves than in leaves expressing EV (Figure 7K). To our surprise, significantly more *P.s.t.* DC3000 D36E grew in *NbNRG2*-expressing leaves than in leaves expressing EV (Supplemental Figure S14E), suggesting that NbNRG2 might play some roles in basal defense in *N. benthamiana*. However, the HopQ1-1-mediated HR (Supplemental Figure S14, F–H) and bacterial growth restriction (Supplemental Figure S14, I and J) were not suppressed by *AtNRG1C* overexpression, indicating that *AtNRG1C* is not able to inhibit *N. benthamiana* NRG1-mediated immunity. Additionally, *NbNRG2* overexpression failed to suppress *chs3-2D*-mediated dwarfism (Supplemental Figure S15, A–C) or the enhanced disease resistance to *H.a.* Noco2 (Supplemental Figure S15D). Since molecular incompatibility among different species or clades was observed in the EDS1–SAG101–NRG1 module (Gantner et al., 2019; Lapin et al., 2019), it is not surprising that NbNRG2 and Brassicaceae NRG1Cs are not functionally exchangeable and that their negative regulation requires molecular compatibility.

Discussion

Truncated NLRs, including TIR only, TN, TIR-unknown domain (TX), CC only, CC-NB (CN), CC-unknown domain (CX), RPW8 only, RPW8-NB (RN), NB-LRR (NL), NB only, and LRR only, are commonly encoded in the genomes of vascular plants (Bai et al., 2002; Meyers et al., 2002, 2003;

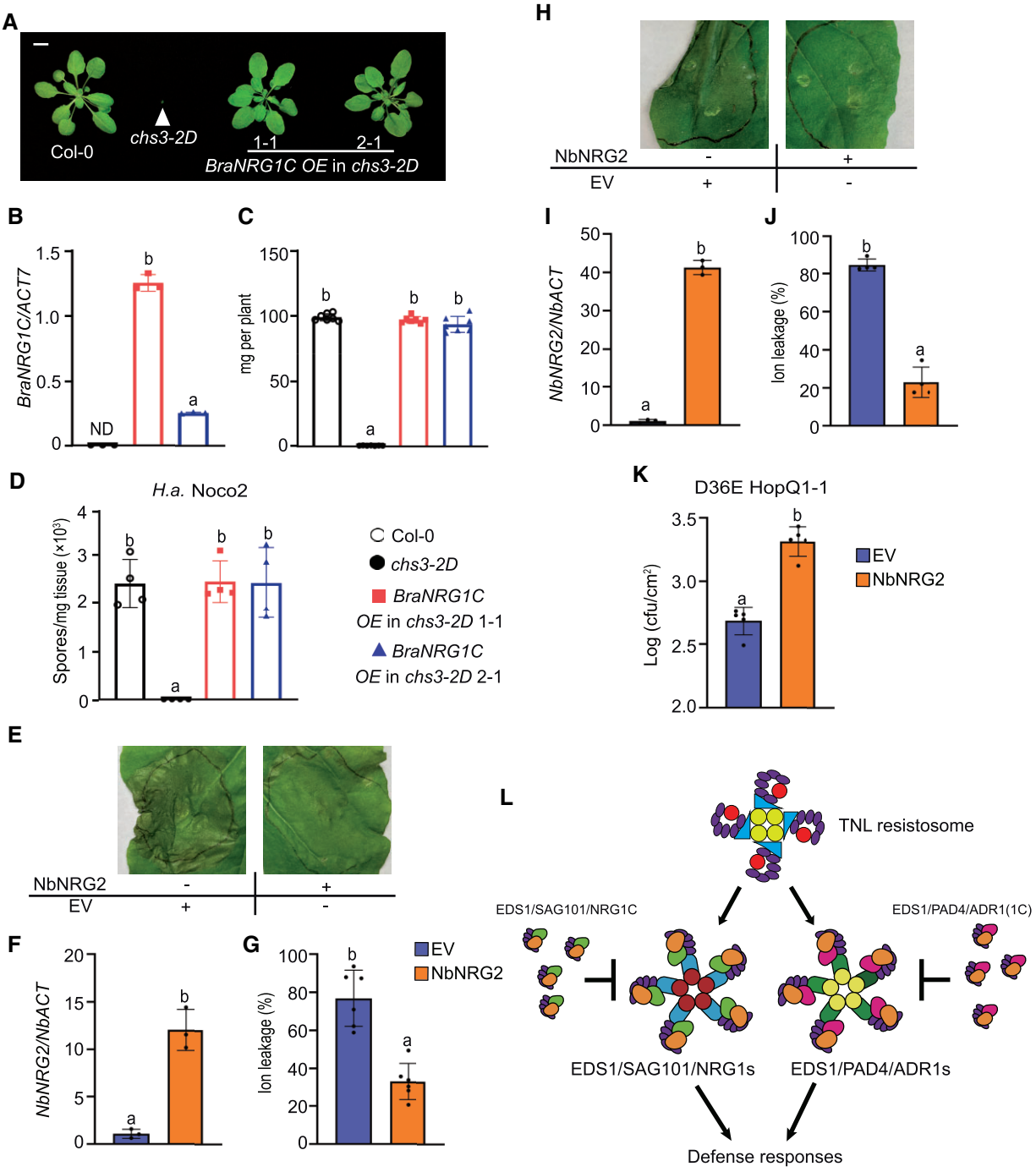

Figure 7 NRG1C-type N-terminally truncated hNLRs from canola (*Brassica napus* cv. Westar) and *N. benthamiana* function similarly to *A. thaliana* NRG1C. A, Morphology of 4-week-old soil-grown plants of Col-0, *chs3-2D*, and two independent transgenic lines of *BraNRG1C OE* in the *chs3-2D* background. Bar = 1 cm. B, *BraNRG1C* gene expression in 2-week-old plate-grown plants, as determined by qRT-PCR. Statistical significance is indicated by different letters ($P < 0.01$). Error bars represent means ± SD ($n = 3$). ND, not detectable. Three independent experiments were carried out with similar results. The color legends are included in D. C, Fresh weights of the plants in (A). Statistical significance is indicated by different letters ($P < 0.01$). Error bars represent means ± SD ($n = 7$). The color legends are included in D. D, Quantification of *H.a.* Noco2 sporulation in the indicated genotypes at 7 dpi with 10^5 spores per ml water. Statistical significance is indicated by different letters ($P < 0.01$). Error bars represent means ± SD ($n = 4$). Three independent experiments were carried out with similar results. E, HR in *N. benthamiana* leaves expressing the indicated proteins at 48 hpi following the infiltration of *P.s.t.* DC3000 D36E HopQ1-1 to deliver HopQ1-1 effector at OD_{600} = 0.2. The photograph was taken at 4 dpi after *P.s.t.* DC3000 D36E HopQ1-1 infiltration. F, *NbNRG2* gene expression in the infiltrated *N. benthamiana* leaves indicated in E, as determined by qRT-PCR (EV-infiltrated leaves served as a control whose *NbNRG2* transcript level was set at 1.0). Samples were collected at 48 hpi with the indicated proteins. Statistical significance is indicated by different letters ($P < 0.01$). Error bars represent means ± SD ($n = 3$). Three independent experiments were carried out with similar results. The color legends are included in G. G, Ion leakage of *N. benthamiana* leaves upon *P.s.t.* DC3000 D36E HopQ1-1 infiltration under the same conditions as in E. Statistical significance is indicated by different letters ($P < 0.01$). Error bars represent means ± SD ($n = 6$). Three independent experiments were carried out with similar results. H, HR in *N. benthamiana* leaves expressing the

Yang et al., 2008; Jacob et al., 2013; Nandety et al., 2013; Baggs et al., 2017; Van de Weyer et al., 2019; Lee and Chae, 2020). A genome-wide survey of *A. thaliana NLR* genes revealed that ~31% of *NLR* genes are truncated (Meyers et al., 2003). Among these, ~90% lack canonical C-terminal domains (Meyers et al., 2002, 2003). Functional characterizations of some C-terminally truncated NLRs have been reported. The TIR-only protein RBA1 can function as an effector sensor and trigger plant immune responses by self-oligomerization (Nishimura et al., 2017). Moreover, the TIR domain in the RBA1 protein possesses NADase activity, which is required to trigger cell death (Wan et al., 2019). Other well-studied TN proteins include TN2 and CHS1. TN2 guards the exocyst complex subunit EXO70B1 (Zhao et al., 2015) and may stabilize the active calcium-dependent protein kinase CPK5 to regulate defense responses (Liu et al., 2017). Interestingly, *TNL SOC3* and *CHS1* cluster together with *TN2* (Zhang et al., 2017; Liang et al., 2019). SOC3 pairs with either CHS1 or TN2 to monitor the absence or overaccumulation of the E3 ligase SAUL1 (Tong et al., 2017; Liang et al., 2019). A recent study found that the LRR-PL (Post-LRR) truncated protein DANGEROUS MIX10 ($DM10^{TueScha-9}$) shows an incompatible interaction with DANGEROUS MIX11 ($DM11^{Cdm-0}$), resulting in hybrid necrosis (Barragan et al., 2020). The chili pepper (*Capsicum baccatum*)-specific truncated CN protein CbCN, missing the LRR domain, positively regulates defense response genes against the fungus *Colletotrichum acutatum* (Son et al., 2021). Therefore, the C-terminally truncated NLRs can often still play positive roles in NLR activation, as they retain the N-terminal signaling domains such as the TIR and NB regions.

In contrast, ~10% of truncated NLRs are N-terminally truncated in *A. thaliana* (Meyers et al., 2003). Although they are widely present in all vascular plant genomes, little is known about their biological significance. In mammalian systems, the Toll-like receptor (TLR) TIR truncations can act as dominant-negative (DN) proteins to dampen immune responses by associating with the same immune activation complexes (Burns et al., 2003; Wells et al., 2006; Padmanabhan et al., 2009). Here, we demonstrated that similar to the truncated TLRs, the N-terminally truncated helper NRG1C lacking the RPW8 CC and part of the NB domain can negatively regulate NRG1A/1B-mediated defense responses. Compared to the DN-TLR examples in the mammalian system, exactly how NRG1C interferes with NRG1A/1B signaling is less clear. As overexpression of a *NRG1C* variant containing a premature stop codon failed to suppress *chs3-2D*-mediated autoimmunity (Figure 6, A–C), and the transcript levels of full-length NRG1A/1B were not affected by overexpression of WT *NRG1C* (Figure 2E; Supplemental Figure S9, B and D), this mechanism unlikely involves transcriptional interference. In addition, NRG1C does not interact with NRG1A/1B (Supplemental Figure S11B), although caution should always be taken with negative protein–protein interaction data.

Sun et al. recently showed that NRG1A associates with the EDS1–SAG101 dimer in an effector-dependent manner (Sun et al., 2021). However, the SAG101–NRG1A/1B signaling branch plays unequal roles in different cases, although EDS1 is required for all tested TNLs (Feys et al., 2005; Xu et al., 2015; Wu et al., 2019, 2021; Sun et al., 2021). For example, SAG101 and NRG1A/1B are fully required for *chs3-2D*-mediated autoimmunity, but they are not needed for CHS1-SOC3 or RPP4-mediated autoimmunity in *saul1-1* or *chs2-1* (Wu et al., 2019). Therefore, the EDS1–SAG101–NRG1A/1B complex is specifically required for some, but not all TNL-mediated immunity. Interestingly, *NRG1C* overexpression phenotypes are identical to those of the *nrg1a nrg1b* double and the *sag101* single mutants. Biochemically, NRG1C can be in complex with EDS1–SAG101 dimers (Figure 6, G and H) (Sun et al., 2021). More NRG1C peptides were detected in the SAG101 IP-MS than NRG1A/1B upon activation of the TNL pair RRS1-RPS4, suggesting that NRG1C might have higher affinity with the EDS1–SAG101 dimer than NRG1A/1B. Taken together, NRG1C may occupy the NRG1A/1B space in the EDS1–SAG101–NRG1A/1B complex, preventing NRG1A/1B interaction with the lipase-like proteins. This would explain the negative interaction data between NRG1A and NRG1C. NRG1C seems to interfere with the EDS1–SAG101 heterodimer via direct association, leading to compromised

Figure 7 (Continued)
indicated proteins at 48 hpi following the infiltration of *Agrobacterium* carrying HopQ1-1 effector at OD_{600} = 0.08. The photographs were taken at 2 dpi after *Agrobacterium* infiltration. Three independent experiments were carried out with similar results. I, *NbNRG2* gene expression in the infiltrated *N. benthamiana* leaves indicated in (H), as determined by qRT-PCR (EV infiltrated leaves served as a control whose *NbNRG2* transcript level was set at 1.0). Samples were collected at 48 hpi with the indicated proteins. Statistical significance is indicated by different letters ($P < 0.01$). Error bars represent means ± SD ($n = 3$). Three independent experiments were carried out with similar results. The color legends are included in K. J, Ion leakage of *N. benthamiana* leaves upon *Agrobacterium* infiltration under the same conditions as in H. Statistical significance is indicated by different letters ($P < 0.01$). Error bars represent means ± SD ($n = 4$). The color legends are included in K. K, Growth of *P.s.t.* DC3000 D36E HopQ1-1 in *N. benthamiana* leaves expressing EV-3FLAG or NbNRG2 for 48 h. After 48 h, the leaves were infiltrated with *P.s.t.* DC3000 D36E HopQ1-1 at OD_{600} = 0.005 and bacterial growth was counted at 4 dpi. Statistical significance is indicated by different letters ($P < 0.01$). Error bars represent means ± SD ($n = 5$). Three independent experiments were carried out with similar results. L, A model depicting the negative regulation of NRG1C downstream of TNL activation in *Arabidopsis*. An effector-induced TNL resistosome with NADase activity (Horsefield et al., 2019; Wan et al., 2019; Ma et al., 2020; Martin et al., 2020; Tian and Li, 2020) signals through two parallel complexes, EDS1–PAD4–ADR1s and EDS1–SAG101–NRG1A/1B, to activate defense responses (Sun et al., 2021; Wu et al., 2021). To avoid over-activation, N-terminally truncated hNLR NRG1C antagonizes immunity mediated by its full-length neighbors NRG1A and NRG1B, while an engineered truncated ADR1 with a similar length to NRG1C [ADR1(1C)] is able to interfere with EDS1–PAD4 dimer to dampen immunity mediated by ADR1s (Wu et al., 2021). Arrows indicate activation, while the "T" signs represent suppression.

NRG1-triggered immunity (Figure 7L). Further biochemical and structural analyses of these proteins are needed to clarify the details of these interactions.

Both NRG1C and ADR1-L3 are N-terminally truncated hNLRs. Although NRG1C negatively regulates some TNL-mediated defense responses, no effect on ADR1-dependent TNL-mediated autoimmunity or pathogen growth was observed upon *ADR1-L3* overexpression (Supplemental Figure S4). In contrast to NRG1C, ADR1-L3 retains the full NB domain (Supplemental Figures S1 and S3). NRG1C homologs are commonly found in Brassicaceae (Figure 1B), whereas an ADR1-L3 homology is only present in *B. stricta* (Supplemental Figure S3). Such an evolutionary difference indicates that ADR1-L3 is likely a pseudogene and thus was lost during evolution. Therefore, for N-terminally truncated NLRs in vascular plant genomes, some may be pseudogenes, and some may have negative functions, as with NRG1C. Although an evolutionary examination may provide an initial hint, functional analysis is needed to determine their exact roles.

Besides *NRG1C* and *ADR1-L3*, five additional N-terminally truncated *NB-LRR* genes are present in the *A. thaliana* Col-0 genome (Supplemental Table S2). AT4G19050, AT5G45510, and AT1G61300 are more closely related to CNLs (Meyers et al., 2003). *AT4G19050* is adjacent to the CN gene *AT4G19060*. *AT5G45510* and the head-to-head arranged CNL *AT5G45520* form a cluster with two other CN genes, *AT5G45490* and *AT5G45440*. *AT1G61310* and the adjacent CNL *AT1G61300* are transcribed in the same direction (Supplemental Table S2). Only two NL proteins, AT5G38350 and AT4G09360, share a similar NB motif with TNLs. *AT5G38350* clusters together with the TIR-only gene *AT5G38344* and the TNL gene *AT5G38340*, while *AT4G09360* resides in the TNL cluster containing TNL *AT4G09430* and *AT4G09420* (Supplemental Table S2). Therefore, clustering of *NL* genes with full-length or C-terminally truncated sNLRs can also be detected in *A. thaliana*. It is possible that the *NL* genes in these clusters play similar roles as *NRG1C* in the *NRG1* cluster, with negative regulatory functions. Additional investigations into the functions of such *NL* genes in *A. thaliana* and other plant species will be of great interest to widen our understanding of NLRs.

Materials and methods

Construction of plasmids

Overexpression constructs of *NRG1C* and *NRG1C*^{T71*} were generated in the *pCambia1305* vector using the KpnI and SpeI restriction sites. The overexpression constructs of *NRG1C* in the *NRG1A D485V* background, *BraNRG1C*, and *NbNRG2* were cloned into the *pBASTA* vector using the KpnI and SpeI restriction sites. The extracted genomic DNA from *Brassica napus* cv. Westar and *N. benthamiana* was used to clone *BraNRG1C* and *NbNRG2* into *pBASTA* using the DraIII and KpnI/SpeI restriction sites, respectively. *DAR5* was cloned into the *pHan* vector using the SfiI restriction site. For the TurboID-based proximity labeling assay, *EDS1*, *SAG101*, *NRG1A*, and *NRG1C* were cloned into *pBASTA-HA-TurboID* using the respective KpnI/SpeI, KpnI/BamHI, KpnI/SpeI, and KpnI/SpeI restriction sites. *NRG1C* and *SAG101* were cloned into *pCambia1300-3FLAG* using the KpnI/SpeI and KpnI/BamHI restriction sites. All genes were driven by the 35S promoter. *pHeeNRG1 (At5g66910-At5g66900)* and *pHeeNRG1C (At5g66890)* were described previously (Wu et al., 2019).

To generate the CRISPR/Cas9 constructs for knocking out *PAD4* and *SAG101*, genomic sequences of *PAD4* and *SAG101* were subjected to CRISPRscan (http://www.crisprscan.org/?page=sequence) to identify the target sequences. The selected sequences were evaluated with Cas-OFFinder (http://www.rgenome.net/cas-offinder/). The *pHEE401E* vector was used to generate the CRISPR/Cas9 constructs as previously described (Wang et al., 2015). All primers used are listed in Supplemental Data Set S1.

Plant materials and growth conditions

A. thaliana snc1, *chs3-2D*, *chs1-2*, *chs2-1*, *chs3-2D nrg1a nrg1b*, *sag101-1*, *snc1 eds1-2*, *snc1 pad4-1*, *snc1 adr1 triple*, *snc1 nrg triple*, *snc1 adr1 triple nrg triple*, *chs1-2 nrg triple*, *chs2-1 nrg triple*, *ADR1-L2 D484V*, and *NRG1A D485V* were previously described (Li et al., 2001; Huang et al., 2010; Bi et al., 2011; Cheng et al., 2011; Roberts et al., 2013; Zbierzak et al., 2013; Dong et al., 2016; Wu et al., 2019).

The *NRG1C* transgenic plants in different backgrounds were generated by transforming *pCambia1305 NRG1C* in the *snc1*, *chs3-2D*, Col-0, *chs1-2*, *ADR1-L2 D484V*, and *chs2-1* backgrounds, *pBastaNRG1C* in the *NRG1A D485V* background or *pBastaNRG1C-HA-TurboID* in *chs3-2D*. The *DAR5* transgenic plants were generated by transforming *pHanDAR5* into the *snc1* or *chs3-2D* background. The *pBastaADR1-L3*, *pBastaBraNRG1C*, *pBastaNRG2* constructs were transformed into either *snc1* or *chs3-2D* to generate the respective transgenic plants. The *pBastaNRG1A-HA-TurboID* construct was transformed into *chs3-2D nrg1a nrg1b* to test their functionality.

The *snc1 sag101-1* double mutant was generated by crossing *snc1* with *sag101-1* (Feys et al., 2005). *snc1 sag101-1* was crossed with *snc1 nrg triple* to generate *snc1 sag101-1 nrg triple* mutant. The CRISPR/Cas9 construct targeting *PAD4* was transformed into *snc1 adr1 triple* (Dong et al., 2016), *snc1 sag101-1*, or *snc1 nrg triple* (Wu et al., 2019) to generate *snc1 pad4-c1 adr1 triple*, *snc1 pad4-c1 sag101-1*, *snc1 pad4-c1 nrg triple* mutants, respectively. The *snc1 sag101-c1 adr1 triple* mutants were generated by transforming the CRISPR/Cas9 construct targeting *SAG101* into the *snc1 adr1 triple* mutant background. Two independent *NRG1C* deletion alleles were generated by transforming the CRISPR/Cas9 construct (Wu et al., 2019) targeting *NRG1C* into the Col-0, *snc1*, and *chs3-2D* backgrounds. *snc1 nrg triple NRG1C OE* and *snc1 sag101-1 NRG1C OE* were generated by crossing *snc1 NRG1C OE* with *snc1 nrg triple* and *snc1 sag101-1*, respectively.

A. thaliana and *N. benthamiana* plants were grown at 22°C under long day (16-h light/8-h dark) or short day (8-h

light/16-h dark) conditions (100 μE; Philips Master TL5 HO 54W/840 bulbs). *chs3-2D* and its transformants were grown at 28°C to suppress the dwarfism and enable seed production.

Stable transformation in *A. thaliana*

The binary constructs were introduced into *Agrobacterium tumefaciens* GV3101 by electroporation and subsequently transformed into *A. thaliana* by the floral dip method (Clough and Bent, 1998). For most transformations, plants were grown at room temperature. For *chs3-2D* transformation, plants were grown at 28°C under a 16-h light/8-h dark regime to reduce autoimmunity. Transformants were selected either on soil by spraying with BASTA (Glufosinate ammonium) or on plates with Hygromycin B. At least 10 transformants were selected for each transformation in the T1 generation, and co-segregation analysis in T2 and T3 generations was carried out to make sure the observed phenotypes were due to the transgene expression.

Transient expression in *N. benthamiana*

Transient *N. benthamiana* expression assays were performed as previously described (Wu et al., 2017b). In brief, *Agrobacteria* carrying the respective constructs were co-infiltrated into 4-week-old *N. benthamiana* leaves. The final OD_{600} for EDS1-HA-TurboID and NRG1A-HA-TurboID was 0.2. The OD_{600} value for GFP-HA-TurboID or SAG101-HA-TurboID was 0.6, whereas OD_{600} = 1.0 was used for strains expressing NRG1C-3FLAG. In Supplemental Figure S14, F–J, NRG1C-3FLAG and EV-3FLAG were infiltrated at OD_{600} = 1.0. In Figure 7, E–K, NbNRG2 and EV-3FLAG were infiltrated at OD_{600} = 0.6. In Supplemental Figure S10, E and F, NRG1C-3FLAG and EV-3FLAG were pre-infiltrated in *N. benthamiana* leaves at OD_{600} = 1.0. At 36 hpi, NRG1A D485V was infiltrated in the indicated area at OD_{600} = 0.2. Each infiltration contained *Agrobacteria p19* to inhibit gene silencing (Lakatos et al., 2004).

Phylogenetic analysis

Putative NRG1A/1B/1C homologs were obtained from Phytozome (Brassicaceae species) and Sol Genomics Network (*N. benthamiana*) using *A. thaliana* NRG1A and NRG1C protein sequences as input, respectively. ADR1 clade hNLRs were excluded from the lists by performing BLAST analysis of ADR1s homologs using AtADR1 protein sequences as input. ZAR1 was used as an outgroup to root the tree. MUSCLE was used for sequence alignment, and a neighbor-joining tree was generated using full-length NRG1C and homologous parts of all other corresponding NRG1 homologs with the JTT model and using 2,000 bootstrap replicates in MEGA version 7.0.

Pathogen infections in *A. thaliana*

Oomycete and bacterial pathogen infection assays were carried out as described previously (Li et al., 2001). In brief, 2-week-old soil-grown seedlings were sprayed with *H.a.* Noco2 or Emwa1 conidia spores at a concentration of 10^5 spores/mL water. After the plants were grown at 18°C for 7 days, sporulation was quantified using a hemocytometer. For bacterial infections, 4-week-old *A. thaliana* plants were infiltrated with bacterial solution at the designated concentrations (see figure legends). Leaf discs were collected and ground on the day of infection (Day 0) and 3 or 4 days later (Day 3/Day 4) (see figure legends). Colony-forming units were calculated after incubation on LB plates with the appropriate antibiotic selections. For the HR assay in *A. thaliana*, 4-week-old soil-grown plants were hand infiltrated with *Pf0-1* carrying pBS46:AvrRPS4 at OD_{600} = 0.2. Ion leakage of infected leaves was monitored at 36 hpi.

qRT-PCR analysis

Approximately 0.05 g of tissue from the aboveground parts of 4-week-old soil-grown or 2-week-old plate-grown seedlings was collected. RNA was extracted from the samples using an RNA isolation kit (Bio Basic; Cat#BS82314). ProtoScript II reverse transcriptase (NEB; Cat#B0368) was used to generate cDNA. qRT-PCR was performed using a SYBR premix kit (TaKaRa, Shiga, Japan, Cat#RR82LR) in a Bio-RAD system (Model No. CFX Connect Optics Module) following the manufacturers' instructions. The primers used are listed in Supplemental Data Set S1.

Agrobacteria infiltration following *P.s.t.* D36E HopQ1-1 infection or HopQ1-1 *Agrobacteria* inoculation

Agrobacteria carrying the respective constructs were infiltrated into 4-week-old *N. benthamiana* leaves expressing EV-FLAG, NRG1C-3FLAG, or NbNRG2. Subsequently, *P.s.t.* DC3000 D36E or *P.s.t.* DC3000 D36E HopQ1-1 was infiltrated in the indicated area of each leaf at 48 h after *Agrobacteria* infiltration at OD_{600} = 0.2 for HR measurement or OD_{600} = 0.005 for bacterial growth measurement. Ion leakage and bacterial growth were measured at 4 days after *P.s.t.* D36E HopQ1-1 infection. *Agrobacteria* expressing HopQ1-1 were infiltrated into the leaves at 48 h after the initial *Agrobacteria* infiltration at OD_{600} = 0.08. Ion leakage was measured at 48 h after HopQ1-1 infiltration.

Ion leakage measurement in *N. benthamiana* and *A. thaliana*

After agrobacteria infiltration, *P.s.t.* DC3000 D36E HopQ1-1 or *Pf0-1* AvrRPS4 infection, *N. benthamiana* leaf discs or whole *A. thaliana* leaves were collected and washed in 10 mL of MilliQ water overnight at room temperature. Ion leakage was measured with a VWR E C METER Model 2052 conductometer. All samples were then autoclaved to measure the total ion leakage.

TurboID-based proximity labeling and co-IP assay in *N. benthamiana*

The co-IP assay was performed as described previously (Wu et al., 2020). In brief, *N. benthamiana* leaves were infiltrated with *Agrobacteria* containing *NRG1C-3FLAG* with either

EDS1-HA-TurboID, *SAG101-HA-TurboID*, or *NRG1A-HA-TurboID*. At 48 hpi, biotin was infiltrated into the leaves. Samples were harvested at 50 hpi and ground into a powder in liquid nitrogen, followed by IP and immunoblot analysis. To test the interaction between NRG1C-3FLAG and SAG101-HA-TurboID, 50 μM of the proteasome inhibitor MG132 was applied with biotin.

TurboID-based proximity labeling and co-IP assay in *A. thaliana*

Whole 2-week-old plate-grown *A. thaliana* transgenic seedlings carrying both *NRG1C-HA-TurboID* and *SAG101-3FLAG* were soaked in water containing 200 μM biotin. Plants were incubated at room temperature for 2 h for labeling and then harvested, followed by IP and immunoblot analysis.

Protein extraction, IP, and immunoblot analysis

An amount of 100 mg samples of soil-grown *A. thaliana* plant leaves or *N. benthamiana* leaves were collected and extracted in extraction buffer (100 mM Tris–HCl pH 8.0, 0.2% SDS, and 2% β-mercaptoethanol). After adding loading buffer to each protein sample, the sample was and boiled for 5 min, followed by immunoblot analysis. Protein abundance was quantified using ImageJ (https://imagej.nih.gov/ij/).

The co-IP assay was performed as previously described (Wu et al., 2017b). In brief, extraction buffer containing 25 mM Tris-HCl pH 7.5, 150 mM NaCl, 1 mM EDTA, 0.15% Nonidet P-40, 10% Glycerol, 1 mM PMSF (Phenylmethylsulfonyl fluoride), 1× Protease Inhibitor Cocktail (Roche, Basel, Switzerland; Cat. #11873580001), and 10 mM DTT (Dithiothreitol) was added to each ground tissue sample. To test the interaction between NRG1C-3FLAG and SAG101-HA-TurboID, 50 μM of the proteasome inhibitor MG132 was added to the extraction buffer. The FLAG-tagged NRG1C and SAG101 proteins were immunoprecipitated using 20 μL M2 beads (Sigma, St Louis, Missouri, USA; Cat. #A2220) for co-IP and biotinylation. HA-tagged proteins were detected using anti-HA antibody (Roche Cat. #11867423001). The anti-FLAG antibody was from Sigma (Cat. #F1804). Biotinylated proteins were detected using Streptavidin-HRP (Abcam, Cambridge, UK; Cat. # ab7403). The previously described anti-EDS1 antibody was generously shared by Dr Jane E. Parker at the Max Planck Institute (Feys et al., 2001).

Statistical analysis

Statistical analysis was performed using one-way ANOVA (Analysis of variance) followed by Tukey's post hoc test. The Scheffé multiple comparison was applied for test correction. Normality tests for all data were performed using SPSS (Statistical Product and Service Solutions). Statistical significance is indicated with different letters. *P*-values and the number of samples (*n*) are detailed in the figure legends. ANOVA tables are provided in Supplemental Data Set S2.

Accession numbers

Sequence data from this article can be found in the GenBank/EMBL libraries under the following accession numbers: NRG1C (AT5G66890); NRG1A (AT5G66900); NRG1B (AT5G66910); ADR1-L3 (AT5G47280); ADR1-L2 (AT5G04720); ADR1 (AT1G33560); ADR1-L1 (AT4G33300); SNC1 (AT4G16890); CHS3 (AT5G17890); DAR5 (AT5G66630); EDS1 (AT3G48090); SAG101 (AT5G14930); PAD4 (AT3G52430); NbNRG1 (Niben101Scf02118g00018.1), NbNRG2 (Niben101Scf03844g01015.1).

Supplemental data

The following materials are available in the online version of this article.

Supplemental Figure S1. Full-length protein sequence alignment of NRG1C and its homologs in different plant species.

Supplemental Figure S2. DAR5 has no effect on *chs3-2D* or *snc1*-mediated autoimmunity.

Supplemental Figure S3. Full-length protein sequence alignment of ADR1-L3 and its homologs in different plant species.

Supplemental Figure S4. No immune-related phenotypes were observed in *ADR1-L3* overexpression lines.

Supplemental Figure S5. Overexpression of *NRG1C* has no effect on *chs1-2* or *chs2-1*-mediated autoimmunity.

Supplemental Figure S6. NRG1C does not affect TNL RPS4, CNL RPS2, *P.s.t* DC3000, or *P.s.t* DC3000 D36E-mediated bacterial growth.

Supplemental Figure S7. Schematic description of CRISPR/Cas9 construct design to delete *PAD4*, *SAG101*, or NRG1C.

Supplemental Figure S8. NRG1C works in the same pathway with the EDS1–SAG101–NRG1A/1B module.

Supplemental Figure S9. Overexpression of *NRG1C* does not affect the transcript or protein levels of full-length NRG1A/1B.

Supplemental Figure S10. NRG1C influences the autoimmunity mediated by *NRG1A D485V*, but not *ADR1-L2 D484V*.

Supplemental Figure S11. NRG1C does not associate with NRG1A.

Supplemental Figure S12. Biotinylation of NRG1C-3FLAG by EDS1-HA-TurboID or SAG101-HA-TurboID in *N. benthamiana* leaves.

Supplemental Figure S13. Overexpression of *NRG1C* does not affect the protein levels of EDS1 or SAG101 in *N. benthamiana*.

Supplemental Figure S14. AtNRG1C does not influence HopQ1-1-mediated HR in *N. benthamiana*.

Supplemental Figure S15. NbNRG2 does not influence *chs3-2D*-mediated autoimmunity.

Supplemental Table S1. The genome arrangements of NRG1C homologs in various plant species.

Supplemental Table S2. The genome arrangements of *NL* truncated genes in *A. thaliana*.

Supplemental Data Set S1. List of primers used in this study.

Supplemental Data Set S2. ANOVA tables.

Acknowledgments

Drs Jeff Dangl, Jane Parker, Marc Nishimura, Brian Staskawicz, Pingtao Ding, Jonathan Jones, Wei Zhang, and Alan Collmer are cordially thanked for generous sharing seeds of the *A. thaliana* mutants, the anti-EDS1 antibody, the *nrg1-1 N. benthamiana* seeds, and *Pseudomonas* strains. Mr Kevin Ao and Dr Paul Kapos are sincerely thanked for careful reading of the manuscript.

Funding

This work was financially supported by funds from CFI-JELF, the Natural Sciences and Engineering Research Council of Canada (NSERC) Discovery and NSERC-CREATE PRoTECT programs to X.Li. and Y.Z. Partial support for the trainees came from scholarships to Z.W. from the Chinese Scholarship Council (CSC) and UBC Dewar Cooper Fund, to L.T. from CSC, to X.Liu. from the MSL Graduate Student Award, and to W.H. from CSC.

Conflict of interest statement. None declared.

References

Adachi H, Contreras MP, Harant A, Wu CH, Derevnina L, Sakai T, Duggan C, Moratto E, Bozkurt TO, Maqbool A, et al. (2019) An N-terminal motif in NLR immune receptors is functionally conserved across distantly related plant species. Elife **8**: e49956

Andolfo G, Villano C, Errico A, Frusciante L, Carputo D, Aversano R, Ercolano MR (2019) Inferring RPW8-NLRs's evolution patterns in seed plants: case study in Vitis vinifera. Planta **251:** 32

Baggs E, Dagdas G, Krasileva KV (2017) NLR diversity, helpers and integrated domains: making sense of the NLR IDentity. Curr Opin Plant Biol **38:** 59–67

Bai J, Pennill LA, Ning J, Lee SW, Ramalingam J, Webb CA, Zhao B, Sun Q, Nelson JC, Leach JE, et al. (2002) Diversity in nucleotide binding site-leucine-rich repeat genes in cereals. Genome Res **12:** 1871–1884

Barragan AC, Collenberg M, Wang J, Lee RRQ, Cher WY, Rabanal FA, Ashkenazy H, Weigel D, Chae E (2020) A truncated singleton NLR causes hybrid necrosis in Arabidopsis thaliana. Mol Biol Evol **38**: 557–574

Bi D, Johnson KC, Zhu Z, Huang Y, Chen F, Zhang Y, Li X (2011) Mutations in an atypical TIR-NB-LRR-LIM resistance protein confer autoimmunity. Front Plant Sci **2:** 71

Bonardi V, Tang S, Stallmann A, Roberts M, Cherkis K, Dangl JL (2011) Expanded functions for a family of plant intracellular immune receptors beyond specific recognition of pathogen effectors. Proc Natl Acad Sci USA **108:** 16463–16468

Burns K, Janssens S, Brissoni B, Olivos N, Beyaert R, Tschopp J (2003) Inhibition of interleukin 1 receptor/Toll-like receptor signaling through the alternatively spliced, short form of MyD88 is due to its failure to recruit IRAK-4. J Exp Med **197:** 263–268

Castel B, Ngou PM, Cevik V, Redkar A, Kim DS, Yang Y, Ding P, Jones JDG (2019) Diverse NLR immune receptors activate defence via the RPW8-NLR NRG1. New Phytol **222:** 966–980

Cheng YT, Li Y, Huang S, Huang Y, Dong X, Zhang Y, Li X (2011) Stability of plant immune-receptor resistance proteins is controlled by SKP1-CULLIN1-F-box (SCF)-mediated protein degradation. Proc Natl Acad Sci USA **108:** 14694–14699

Clough SJ, Bent AF (1998) Floral dip: a simplified method for Agrobacterium-mediated transformation of Arabidopsis thaliana. Plant J **16:** 735–743

Collier SM, Hamel LP, Moffett P (2011) Cell death mediated by the N-terminal domains of a unique and highly conserved class of NB-LRR protein. Mol Plant Microbe Interact **24:** 918–931

Couto D, Zipfel C (2016) Regulation of pattern recognition receptor signalling in plants. Nat Rev Immunol **16:** 537–552

Cui H, Tsuda K, Parker JE (2015) Effector-triggered immunity: from pathogen perception to robust defense. Annu Rev Plant Biol **66:** 487–511

Dong OX, Tong M, Bonardi V, El Kasmi F, Woloshen V, Wünsch LK, Dangl JL, Li X (2016) TNL-mediated immunity in Arabidopsis requires complex regulation of the redundant ADR1 gene family. New Phytol **210:** 960–973

Feys BJ, Moisan LJ, Newman MA, Parker JE (2001) Direct interaction between the Arabidopsis disease resistance signaling proteins, EDS1 and PAD4. EMBO J **20:** 5400–5411

Feys BJ, Wiermer M, Bhat RA, Moisan LJ, Medina-Escobar N, Neu C, Cabral A, Parker JE (2005) Arabidopsis SENESCENCE-ASSOCIATED GENE101 stabilizes and signals within an ENHANCED DISEASE SUSCEPTIBILITY1 complex in plant innate immunity. Plant Cell **17:** 2601–2613

Gabriëls SH, Takken FL, Vossen JH, de Jong CF, Liu Q, Turk SC, Wachowski LK, Peters J, Witsenboer HM, de Wit PJ, et al. (2006) CDNA-AFLP combined with functional analysis reveals novel genes involved in the hypersensitive response. Mol Plant Microbe Interact **19:** 567–576

Gabriëls SH, Vossen JH, Ekengren SK, van Ooijen G, Abd-El-Haliem AM, van den Berg GC, Rainey DY, Martin GB, Takken FL, de Wit PJ, et al. (2007) An NB-LRR protein required for HR signalling mediated by both extra- and intracellular resistance proteins. Plant J **50:** 14–28

Gantner J, Ordon J, Kretschmer C, Guerois R, Stuttmann J (2019) An EDS1-SAG101 complex is essential for TNL-mediated immunity in Nicotiana benthamiana Plant Cell **31:** 2456–2474

Gao Y, Wang W, Zhang T, Gong Z, Zhao H, Han GZ (2018) Out of water: the origin and early diversification of plant. Plant Physiol **177:** 82–89

Guo YL, Fitz J, Schneeberger K, Ossowski S, Cao J, Weigel D (2011) Genome-wide comparison of nucleotide-binding site-leucine-rich repeat-encoding genes in Arabidopsis. Plant Physiol **157:** 757–769

Horsefield S, Burdett H, Zhang X, Manik MK, Shi Y, Chen J, Qi T, Gilley J, Lai JS, Rank MX, et al. (2019) NAD + cleavage activity by animal and plant TIR domains in cell death pathways. Science **365:** 793–799

Howard BE, Hu Q, Babaoglu AC, Chandra M, Borghi M, Tan X, He L, Winter-Sederoff H, Gassmann W, Veronese P, et al. (2013) High-throughput RNA sequencing of pseudomonas-infected Arabidopsis reveals hidden transcriptome complexity and novel splice variants. PLoS One **8:** e74183

Huang X, Li J, Bao F, Zhang X, Yang S (2010) A gain-of-function mutation in the Arabidopsis disease resistance gene RPP4 confers sensitivity to low temperature. Plant Physiol **154:** 796–809

Jacob F, Vernaldi S, Maekawa T (2013) Evolution and conservation of plant NLR functions. Front Immunol **4:** 297

Jones JDG, Dangl JL (2006) The plant immune system. Nature **444**: 323–329

Jones JD, Vance RE, Dangl JL (2016) Intracellular innate immune surveillance devices in plants and animals. Science **354**: aaf6395

Jubic LM, Saile S, Furzer OJ, El Kasmi F, Dangl JL (2019) Help wanted: helper NLRs and plant immune responses. Curr Opin Plant Biol **50:** 82–94

Krasileva KV (2019) The role of transposable elements and DNA damage repair mechanisms in gene duplications and gene fusions in plant genomes. Curr Opin Plant Biol **48:** 18–25

Lakatos L, Szittya G, Silhavy D, Burgyán J (2004) Molecular mechanism of RNA silencing suppression mediated by p19 protein of tombusviruses. EMBO J **23:** 876–884

Lapin D, Kovacova V, Sun X, Dongus JA, Bhandari D, von Born P, Bautor J, Guarneri N, Rzemieniewski J, Stuttmann J, et al. (2019) A coevolved EDS1-SAG101-NRG1 module mediates cell death signaling by TIR-domain immune receptors. Plant Cell **31:** 2430–2455

Lee RRQ, Chae E (2020) Variation patterns of NLR clusters in *Arabidopsis thaliana* genomes. Plant Commun **1:** 100089

Li X, Clarke JD, Zhang Y, Dong X (2001) Activation of an EDS1-mediated R-gene pathway in the snc1 mutant leads to constitutive, NPR1-independent pathogen resistance. Mol Plant Microbe Interact **14:** 1131–1139

Liang W, van Wersch S, Tong M, Li X (2019) TIR-NB-LRR immune receptor SOC3 pairs with truncated TIR-NB protein CHS1 or TN2 to monitor the homeostasis of E3 ligase SAUL1. New Phytol **221:** 2054–2066

Liu N, Hake K, Wang W, Zhao T, Romeis T, Tang D (2017) CALCIUM-DEPENDENT PROTEIN KINASE5 associates with the truncated NLR protein TIR-NBS2 to contribute to *exo70B1*-mediated immunity. Plant Cell **29:** 746–759

Lu X, Kracher B, Saur IM, Bauer S, Ellwood SR, Wise R, Yaeno T, Maekawa T, Schulze-Lefert P (2016) Allelic barley MLA immune receptors recognize sequence-unrelated avirulence effectors of the powdery mildew pathogen. Proc Natl Acad Sci USA **113:** E6486–E6495

Ma S, Lapin D, Liu L, Sun Y, Song W, Zhang X, Logemann E, Yu D, Wang J, Jirschitzka J, et al. (2020) Direct pathogen-induced assembly of an NLR immune receptor complex to form a holoenzyme. Science **370**: eabe3069

Mago R, Zhang P, Vautrin S, Šimková H, Bansal U, Luo MC, Rouse M, Karaoglu H, Periyannan S, Kolmer J, et al. (2015) The wheat Sr50 gene reveals rich diversity at a cereal disease resistance locus. Nat Plants **1:** 15186

Marone D, Russo MA, Laidò G, De Leonardis AM, Mastrangelo AM (2013) Plant nucleotide binding site-leucine-rich repeat (NBS-LRR) genes: active guardians in host defense responses. Int J Mol Sci **14:** 7302–7326

Martin R, Qi T, Zhang H, Liu F, King M, Toth C, Nogales E, Staskawicz BJ (2020) Structure of the activated ROQ1 resistosome directly recognizing the pathogen effector XopQ. Science **370**: eabd9993

Meyers BC, Morgante M, Michelmore RW (2002) TIR-X and TIR-NBS proteins: two new families related to disease resistance TIR-NBS-LRR proteins encoded in Arabidopsis and other plant genomes. Plant J **32:** 77–92

Meyers BC, Kozik A, Griego A, Kuang H, Michelmore RW (2003) Genome-wide analysis of NBS-LRR-encoding genes in Arabidopsis. Plant Cell **15:** 809–834

Michelmore RW, Meyers BC (1998) Clusters of resistance genes in plants evolve by divergent selection and a birth-and-death process. Genome Res **8:** 1113–1130

Nandety RS, Caplan JL, Cavanaugh K, Perroud B, Wroblewski T, Michelmore RW, Meyers BC (2013) The role of TIR-NBS and TIR-X proteins in plant basal defense responses. Plant Physiol **162:** 1459–1472

Nishimura MT, Anderson RG, Cherkis KA, Law TF, Liu QL, Machius M, Nimchuk ZL, Yang L, Chung EH, El Kasmi F, et al. (2017) TIR-only protein RBA1 recognizes a pathogen effector to regulate cell death in *Arabidopsis*. Proc Natl Acad Sci USA **114:** E2053–E2062

Padmanabhan M, Cournoyer P, Dinesh-Kumar SP (2009) The leucine-rich repeat domain in plant innate immunity: a wealth of possibilities. Cell Microbiol **11:** 191–198

Peart JR, Mestre P, Lu R, Malcuit I, Baulcombe DC (2005) NRG1, a CC-NB-LRR protein, together with N, a TIR-NB-LRR protein, mediates resistance against tobacco mosaic virus. Curr Biol **15:** 968–973

Qi T, Seong K, Thomazella DPT, Kim JR, Pham J, Seo E, Cho MJ, Schultink A, Staskawicz BJ (2018) NRG1 functions downstream of EDS1 to regulate TIR-NLR-mediated plant immunity in *Nicotiana benthamiana*. Proc Natl Acad Sci USA **115:** E10979–E10987

Rathjen JP, Dodds PN (2017) Dancing with the stars: an asterid NLR family. Trends Plant Sci **22:** 1003–1005

Rietz S, Stamm A, Malonek S, Wagner S, Becker D, Medina-Escobar N, Vlot AC, Feys BJ, Niefind K, Parker JE (2011) Different roles of enhanced disease susceptibility1 (EDS1) bound to and dissociated from Phytoalexin Deficient4 (PAD4) in Arabidopsis immunity. New Phytol **191:** 107–119

Roberts M, Tang S, Stallmann A, Dangl JL, Bonardi V (2013) Genetic requirements for signaling from an autoactive plant NB-LRR intracellular innate immune receptor. PLoS Genet **9:** e1003465

Saile SC, Jacob P, Castel B, Jubic LM, Salas-Gonzáles I, Bäcker M, Jones JDG, Dangl JL, El Kasmi F (2020) Two unequally redundant "helper" immune receptor families mediate Arabidopsis thaliana intracellular "sensor" immune receptor functions. PLoS Biol **18:** e3000783

Saucet SB, Ma Y, Sarris PF, Furzer OJ, Sohn KH, Jones JD (2015) Two linked pairs of Arabidopsis TNL resistance genes independently confer recognition of bacterial effector AvrRps4. Nat Commun **6:** 6338

Schultink A, Qi T, Lee A, Steinbrenner AD, Staskawicz B (2017) Roq1 mediates recognition of the Xanthomonas and Pseudomonas effector proteins XopQ and HopQ1. Plant J **92:** 787–795

Serra H, Choi K, Zhao X, Blackwell AR, Kim J, Henderson IR (2018) Interhomolog polymorphism shapes meiotic crossover within the Arabidopsis RAC1 and RPP13 disease resistance genes. PLoS Genet **14:** e1007843

Shao ZQ, Xue JY, Wu P, Zhang YM, Wu Y, Hang YY, Wang B, Chen JQ (2016) Large-scale analyses of angiosperm nucleotide-binding site-leucine-rich repeat genes reveal three anciently diverged classes with distinct evolutionary patterns. Plant Physiol **170:** 2095–2109

Son S, Kim S, Lee KS, Oh J, Choi I, Do JW, Yoon JB, Han J, Park SR (2021) The capsicum baccatum -specific truncated NLR protein CbCN enhances the innate immunity against Colletotrichum acutatum. Int J Mol Sci **22**: 7672

Sun X, Lapin D, Feehan JM, Stolze SC, Kramer K, Dongus JA, Rzemieniewski J, Blanvillain-Baufumé S, Harzen A, Bautor J, et al. (2021) Pathogen effector recognition-dependent association of NRG1 with EDS1 and SAG101 in TNL receptor immunity. Nat Commun **12:** 3335

Tamborski J, Krasileva KV (2020) Evolution of plant NLRs: from natural history to precise modifications. Annu Rev Plant Biol **71:** 355–378

Tan X, Meyers BC, Kozik A, West MA, Morgante M, St Clair DA, Bent AF, Michelmore RW (2007) Global expression analysis of nucleotide binding site-leucine rich repeat-encoding and related genes in Arabidopsis. BMC Plant Biol **7:** 56

Thomas WJ, Thireault CA, Kimbrel JA, Chang JH (2009) Recombineering and stable integration of the Pseudomonas syringae pv. syringae 61 hrp/hrc cluster into the genome of the soil bacterium Pseudomonas fluorescens Pf0-1. Plant J **60:** 919–928

Tian L, Li X (2020) Enzyme formation by immune receptors. Science **370:** 1163–1164

Tong M, Kotur T, Liang W, Vogelmann K, Kleine T, Leister D, Brieske C, Yang S, Lüdke D, Wiermer M, et al. (2017) E3 ligase SAUL1 serves as a positive regulator of PAMP-triggered immunity and its homeostasis is monitored by immune receptor SOC3. New Phytol **215:** 1516–1532

Van de Weyer AL, Monteiro F, Furzer OJ, Nishimura MT, Cevik V, Witek K, Jones JDG, Dangl JL, Weigel D, Bemm F (2019) A species-wide inventory of NLR genes and alleles in Arabidopsis thaliana. Cell **178:** 1260–1272.e1214

van Wersch S, Li X (2019) Stronger when together: clustering of plant NLR disease resistance genes. Trends Plant Sci **24:** 688–699

Wan L, Essuman K, Anderson RG, Sasaki Y, Monteiro F, Chung EH, Osborne Nishimura E, DiAntonio A, Milbrandt J, et al. (2019) TIR domains of plant immune receptors are NAD + -cleaving enzymes that promote cell death. Science **365:** 799–803

Wang Y, Zhang Y, Wang Z, Zhang X, Yang S (2013) A missense mutation in CHS1, a TIR-NB protein, induces chilling sensitivity in Arabidopsis. Plant J **75:** 553–565

Wang ZP, Xing HL, Dong L, Zhang HY, Han CY, Wang XC, Chen QJ (2015) Egg cell-specific promoter-controlled CRISPR/Cas9 efficiently generates homozygous mutants for multiple target genes in Arabidopsis in a single generation. Genome Biol **16:** 144

Wei HL, Chakravarthy S, Mathieu J, Helmann TC, Stodghill P, Swingle B, Martin GB, Collmer A (2015) Pseudomonas syringae pv. tomato DC3000 type III secretion effector polymutants reveal an interplay between HopAD1 and AvrPtoB. Cell Host Microbe **17:** 752–762

Wells CA, Chalk AM, Forrest A, Taylor D, Waddell N, Schroder K, Himes SR, Faulkner G, Lo S, Kasukawa T, et al. (2006) Alternate transcription of the Toll-like receptor signaling cascade. Genome Biol **7:** R10

Wicker T, Yahiaoui N, Keller B (2007) Illegitimate recombination is a major evolutionary mechanism for initiating size variation in plant resistance genes. Plant J **51:** 631–641

Wu CH, Belhaj K, Bozkurt TO, Birk MS, Kamoun S (2016) Helper NLR proteins NRC2a/b and NRC3 but not NRC1 are required for Pto-mediated cell death and resistance in Nicotiana benthamiana. New Phytol **209:** 1344–1352

Wu CH, Abd-El-Haliem A, Bozkurt TO, Belhaj K, Terauchi R, Vossen JH, Kamoun S (2017a) NLR network mediates immunity to diverse plant pathogens. Proc Natl Acad Sci USA **114:** 8113–8118

Wu Z, Huang S, Zhang X, Wu D, Xia S, Li X (2017b) Regulation of plant immune receptor accumulation through translational repression by a glycine-tyrosine-phenylalanine (GYF) domain protein. Elife **6**: e23684

Wu Z, Tong M, Tian L, Zhu C, Liu X, Zhang Y, Li X (2020) Plant E3 ligases SNIPER1 and SNIPER2 broadly regulate the homeostasis of sensor NLR immune receptors. EMBO J **39:** e104915

Wu Z, Li M, Dong OX, Xia S, Liang W, Bao Y, Wasteneys G, Li X (2019) Differential regulation of TNL-mediated immune signaling by redundant helper CNLs. New Phytol **222:** 938–953

Wu Z, Tian L, Liu X, Zhang Y, Li X (2021) TIR signal promotes interactions between lipase-like proteins and ADR1-L1 receptor and ADR1-L1 oligomerization. Plant Physiol **187:** 681–686

Xu F, Zhu C, Cevik V, Johnson K, Liu Y, Sohn K, Jones JD, Holub EB, Li X (2015) Autoimmunity conferred by chs3-2D relies on CSA1, its adjacent TNL-encoding neighbour. Sci Rep **5:** 8792

Yang S, Zhang X, Yue JX, Tian D, Chen JQ (2008) Recent duplications dominate NBS-encoding gene expansion in two woody species. Mol Genet Genomics **280:** 187–198

Zbierzak AM, Porfirova S, Griebel T, Melzer M, Parker JE, Dörmann P (2013) A TIR-NBS protein encoded by Arabidopsis Chilling Sensitive 1 (CHS1) limits chloroplast damage and cell death at low temperature. Plant J **75:** 539–552

Zhang Y, Wang Y, Liu J, Ding Y, Wang S, Zhang X, Liu Y, Yang S (2017) Temperature-dependent autoimmunity mediated by chs1 requires its neighboring TNL gene SOC3. New Phytol **213:** 1330–1345

Zhang Y, Song G, Lal NK, Nagalakshmi U, Li Y, Zheng W, Huang PJ, Branon TC, Ting AY, Walley JW, et al. (2019) TurboID-based proximity labeling reveals that UBR7 is a regulator of N NLR immune receptor-mediated immunity. Nat Commun **10:** 3252

Zhao T, Rui L, Li J, Nishimura MT, Vogel JP, Liu N, Liu S, Zhao Y, Dangl JL, Tang D (2015) A truncated NLR protein, TIR-NBS2, is required for activated defense responses in the exo70B1 mutant. PLoS Genet **11:** e1004945

Zhong Y, Cheng ZM (2016) A unique RPW8-encoding class of genes that originated in early land plants and evolved through domain fission, fusion, and duplication. Sci Rep **6:** 32923